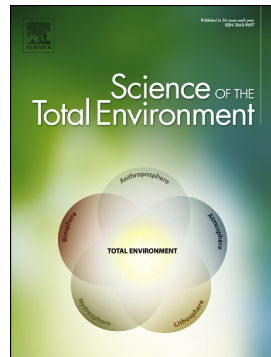


Journal Pre-proof

Chemical and isotopic characteristics of PM2.5 over New Delhi from September 2014 to May 2015: Evidences for synergy between air-pollution and meteorological changes

Ravi Sawlani, Rajesh Agnihotri, C. Sharma



PII: S0048-9697(20)36496-2

DOI: <https://doi.org/10.1016/j.scitotenv.2020.142966>

Reference: STOTEN 142966

To appear in: *Science of the Total Environment*

Received date: 30 June 2020

Revised date: 8 September 2020

Accepted date: 6 October 2020

Please cite this article as: R. Sawlani, R. Agnihotri and C. Sharma, Chemical and isotopic characteristics of PM2.5 over New Delhi from September 2014 to May 2015: Evidences for synergy between air-pollution and meteorological changes, *Science of the Total Environment* (2020), <https://doi.org/10.1016/j.scitotenv.2020.142966>

This is a PDF file of an article that has undergone enhancements after acceptance, such as the addition of a cover page and metadata, and formatting for readability, but it is not yet the definitive version of record. This version will undergo additional copyediting, typesetting and review before it is published in its final form, but we are providing this version to give early visibility of the article. Please note that, during the production process, errors may be discovered which could affect the content, and all legal disclaimers that apply to the journal pertain.

Chemical and isotopic characteristics of PM_{2.5} over New Delhi from September 2014 to May 2015: Evidences for synergy between air-pollution and meteorological changes

Ravi Sawlani^{1,2}, Rajesh Agnihotri^{2,3*}, C. Sharma^{1,2}

¹CSIR-National Physical Laboratory, K.S. Krishnan Marg, New Delhi, 110012, India

²Academy of Scientific and Innovative Research (AcSIR), CSIR National Physical Laboratory Campus, New Delhi 110012, India

³Birbal Sahni Institute of Palaeosciences 53, University Road, Lucknow, 226007, India

*Corresponding author's Email: rajagni9@gmail.com

Abstract

The capital city of India, New Delhi, is experiencing serious PM_{2.5} pollution in the form of recurrent hazy skies and smoky fog (SMOG) episodes in recent years. Besides source-emission strengths, frequency and time-spans of these air-pollution episodes are uncertain due to variable urban meteorological influences, preventing the formation of a cohesive policy to tackle air-quality degradation. About 70% mass of PM_{2.5} particle is composed of Carbon (C), Nitrogen (N), and Sulphur (S) and, hence, their mass concentrations along with their stable isotopic imprints (viz. □¹³C_{PM2.5}, □¹⁵N_{PM2.5} and □³⁴S_{PM2.5}) provide powerful tools to gain insights into complex aerosol chemistry. This study presents the aforementioned data generated for PM_{2.5} collected from New Delhi covering full post-monsoon, winter, and summer months of 2014-15. Temporal variability in the generated dataset was analysed with variabilities in atmospheric concentrations of key gaseous species (NH₃, NO_x, and SO₂) and meteorological indices. The highest PM_{2.5} concentrations were observed in winter months with enhanced aerosol N and S concentrations. Active biomass (crop-residue) burning in the northwest Indo-Gangetic Plains (IGP) appears to be the major source of aerosol TC for post-monsoon and winter months in addition to emission sources from the combustion of bio- and fossil-fuels. Aerosol TN contents appear to be largely impacted by ambient ammonia emissions, especially during winter. Aerosol TS contents could be manifested by emissions from coal combustion, road dust, and biogenic sulphur. Total C+N+S contents of PM_{2.5} showed significant

negative correlations with surface solar radiation and air-visibility. Both $\square^{15}\text{N}_{\text{PM}2.5}$ and $\delta^{34}\text{S}_{\text{PM}2.5}$ values show remarkable correlations with air-quality and meteorological parameters during winter months demonstrating considerable secondary cycling. Cluster analysis and concentrated weighted wind trajectories over New Delhi for the study-period showed ~64% and ~58% of air mass trajectories from the northwest (Punjab-Haryana) region during post-monsoon and winter months respectively.

Keywords:

PM_{2.5} aerosols; Stable isotopes of Carbon-Nitrogen-Sulphur; Biomass burning; Air-visibility; Ammonia emissions

1. Introduction

Airborne fine particulate matter (PM_{2.5}) is a major air-pollutant carrying several toxic pollutants in the lower atmosphere and thereby poses serious threats to regional air quality, human health, climate, and various human activities in general (Marrison and Yin, 2000; Seinfeld and Pandis, 2016; Anderson, 2003; Pope and Dockery, 2006). Both natural and anthropogenic emissions are responsible for the creation of PM_{2.5} particles. PM_{2.5} are mainly formed by oxidation/ destruction of the primary aerosols during the long range transportation of pollutants along with the gas to particle conversions of N and S species (Hillquist et al., 2009; Pokhrel et al., 2015). In Southeast Asia, many of the urban centres like New Delhi are experiencing high concentrations of atmospheric PM_{2.5} almost throughout the year, causing serious respiratory and cardiopulmonary diseases in the resident population like asthma, bronchitis (Chowdhury et al., 2019; Dockery et al., 1993; Pope III, 2002). New Delhi, the political capital of India is situated in the middle of IGP and receives aerosol particles (both coarse as well as fine) from a variety of natural (*e.g.* windblown dust from the Thar Desert) and anthropogenic sources (such as fossil fuel and biomass burning, industrial and vehicular emissions, coal-burning for power generation, road dust, cracker bursting activities during festivals, etc.). These particles could

be laden with a variety of toxic and sticky pollutants inducing thick haze/ smoky fog (SMOG) especially in winters and cause allergic diseases (Reinmuth-Selzle et al., 2017; Sawlani et al., 2019). Being the capital region of densely populated India, anthropogenic developmental and industrial activities in and around New Delhi continues to expand in all directions. A total of 24 districts in three neighbouring states of Delhi i.e. Haryana, Uttar Pradesh, and Rajasthan constitute the National Capital Region (NCR) of India and air-quality degradation remains a most compelling environmental issue for the entire NCR region (Ghosh et al., 2015). Degradation of regional air-quality over New Delhi and NCR has worsened from ‘very poor’ to ‘serious’ category owing to frequent recurrence of haze/ SMOG episodes spanning from few days to week-long durations right after the end of monsoon season. The late withdrawal of Indian southwest monsoon and extended periods of crop-residue burning in northwest India (Punjab and Haryana states) have also been considered as potential contributing factors for air-quality degradation over New Delhi and NCR at times stretching further up to the entire IGP region comprising of Uttar Pradesh, Bihar and West Bengal states (Badarinath et al., 2009; Sawlani et al., 2019). Degraded air-quality (marked by poor air-visibility) especially during post-monsoon and early winter periods force the city-administration to shut down schools, open air gatherings, cancelling cricket matches, flight diversions/ cancellations, interruptions in train and road traffic collectively incurring heavy economic losses (Subramanian, 2016). Several policy measures have been attempted in Delhi to mitigate/ reduce air pollution; such as Odd-Even rule for private four-wheelers, sprinkling water on trees with water cannons, and installing SMOG towers at busy heavily polluted areas. So far, none of the attempted measures have been found to be able to contain airquality degradation, and PM_{2.5} pollution continues to enhance every year, especially during post monsoon and winter months. Major causes for this ineffectiveness of policy measures include: (i) insufficient knowledge of strengths of sources- responsible for enhancing PM_{2.5} in ambient air, and

(ii) limited knowledge of secondary atmospheric processes working in synergy with urban meteorological conditions that aggravate PM_{2.5} pollution. Besides enhancing the information of dominant sources contributing to the build-up of airborne particles, knowledge of secondary atmospheric processes , oxidation pathways, photolytic destructions, and gas to particle conversions are key to developing meteorology–atmospheric chemistry coupled models (Baklanov et al., 2018). In addition, the effects of atmospheric particle composition on regional weather need to be properly understood (Aggarwal et al., 2013; Aggarwal and Kawamura, 2008; Agnihotri, 2015; Agnihotri et al., 2011; Kawamura et al., 2004; Narukawa et al., 2008; Pavuluri et al., 2010; Rastogi et al., 2020; Sawlani et al., 2019).

As stated earlier, C, N, and S contribute ~70% of PM_{2.5} particle mass (Pöschl, 2005), their quantitative propositions (mass concentrations) along with their stable isotopic imprints ($\square^{13}\text{C}_{\text{PM}2.5}$, $\square^{15}\text{N}_{\text{PM}2.5}$ and $\square^{34}\text{S}_{\text{PM}2.5}$) can greatly assist in identification of major sources responsible and insights into (i) complex secondary processes *e.g.* gas to particle conversions and (ii) dominant meteorological influences. Detailed time-series data capturing seasonal variability in these basic chemical constituents and their isotopic composition can thus greatly help to garner insights into synergies between air pollution and meteorological factors. The Central Pollution Control Board of India (CPCB) is regularly monitoring and recording variability in major gaseous pollutants' ambient concentrations (*e.g.* NH₃, NO_x and SO₂) while India Meteorological Department monitors the major meteorological parameters (*e.g.* temperature, relative humidity, air visibility, surface solar radiation etc.). But limited studies so far, have attempted to investigate meteorological influences on fine-aerosol particle chemistry covering major transition periods when air quality is known to deteriorate badly in Delhi.

In this study, we carried out a detailed sampling of ambient PM_{2.5} particles from a central New Delhi location and quantified aerosol C, N, and S components and their stable isotopic compositions. We investigated variability in the generated aerosols data in the realm of the same day recorded concentration data of ambient NH₃, NO_x, and SO₂ along with the aforementioned major meteorological parameters. Earlier studies (Malm et al., 1996; Ramana et al., 2004; Sawlani et al., 2019; Tiwari et al., 2011) have demonstrated that meteorological transition periods, especially from post-monsoon to winter period in north India are marked by abrupt changes in wind-directions with a significant reduction in wind-speeds; these conditions often coincide with sudden drops and rise in ambient temperatures and relative humidity respectively which collectively favour the build-up of elevated ambient PM_{2.5} concentrations. These enhanced PM_{2.5} levels in the lower atmosphere result in very low visibilities and thick haze/ SMOG occurrences (Sawlani et al., 2019).

In order to probe the probable causes of such air-pollution episodes, we examined the generated and monitored data in three seasons namely post-monsoon (September, October and November), winter (December, January, and February), and spring-summer (March, April, and May). To identify geographic sources of winds blowing over the sampling site, we carried out multivariate statistical analysis (clustering) of backward winds (for three days) and also evaluated concentration-weighted wind trajectories. Information congregated in this synthesis for New Delhi location could be potentially utilized for other land-locked urban centres (i.e. metro cities) of south Asia by agencies involved in developing coupled chemistry–meteorology-climate models for numerical air-quality and weather predictions.

2. Materials and Methods

2.1 Sampling Site and Sample collection

New Delhi is situated in the tropical climate zone which experiences extreme changes in the meteorological parameters having minimum temperature as low as $\sim 0\text{--}2^\circ\text{C}$ in winters with nearly 100% relative humidity and domination of the northwest (NW) winds, whereas in summers, the maximum temperature reaches to $\sim 45^\circ\text{C}$ dominated by the southwest (SW) dry winds.

$\text{PM}_{2.5}$ sampling was carried out at the rooftop of TEC Building, CSIR-National Physical Laboratory ($28^\circ 38' \text{N}$, $77^\circ 10' \text{E}$; ~ 15 m from ground level), situated at a central location of New Delhi. The sample collection site is surrounded by the heavy roadside traffic on one side (east) and vegetation covered agricultural fields (belonging to Indian Agricultural Research Institute, Pusa) from the other three sides (Fig.1). During the entire study period, a total of 117 $\text{PM}_{2.5}$ aerosol samples were collected with a frequency of $\sim 10\text{--}12$ samples per month from September 2014 to May 2015 using a low volume air sampler (*Ecotech®, Australia*) having a fixed flow rate of 3 litre min^{-1} . The collection of each sample was carried out for 24 hours duration, adhering to the CPCB guidelines. All samples were collected on circular punches (diameter $\varphi=4 / 1.1\text{ mm}$) of tissue quartz filters (*Pall Life Sciences*) and all the filters used for sample collection were pre-baked and desiccated before weighing on an analytical balance (*Sartorius®*) before and after the sampling. Proper safety gears (gloves, clean laminar flow bench, etc.) were used with minimal human handling of $\text{PM}_{2.5}$ filter samples to avoid any possible contamination. The generated chemical and isotopic dataset of ambient $\text{PM}_{2.5}$ sufficiently covers full post-monsoon, winter, spring-summer months. We attempted to collect ambient $\text{PM}_{2.5}$ samples at a regular interval to maintain data uniformity (in the temporal domain) for the representation of the meteorological transition periods during this nine month-long period.

Simultaneously recorded data of meteorological (MET) parameters (e.g. ambient temperature,

humidity, and surface solar radiation) and relevant gaseous emissions (NH_3 , NO_x , and SO_2) were obtained from the official website of the CPCB, (<http://www.cpcb.gov.in/CAAQM/frmUserAvgReportCriteria.aspx>) and averaged data for 24 hours were used for the inter-comparison purpose. The daily average of air-visibility data was obtained from National Centers for Environmental Information (NCEI), USA. Air-visibility data is taken for the Indira Gandhi International Airport (~12 km away from sample collection site at NPL, New Delhi).

2.2 Methodology used for stable isotope analysis

Chemical constituents of $\text{PM}_{2.5}$ particles i.e. total C, total N, and total S along with their isotopic compositions ($\square^{13}\text{C}$, $\square^{15}\text{N}$, and $\square^{34}\text{S}$ values) were measured on circular punches (diameter $\varphi\sim 1$ cm) cut from aerosol filters with the help of a custom made (pre-clean) dye. Generally two to three aliquots were cut and placed into the clean circular tin cups. After placing the sample into tin cups, they were closed from all sides and pressed into round pellets using flat-tipped clean stainless tweezers. The total procedure was carried out in a laminar flow bench under a clean air environment ensuring contamination-free environment. For analysis, pressed pellets were dropped into the combustion reactor of the Elemental Analyzer (EA; *Pyrocube®*, Elementar GmbH Germany) coupled with IRMS (*Isoprime 100®*, Isoprime UK) using an auto-sampler. Sample pellets were combusted in a combustion reactor filled with tungsten oxide (WO_3) catalyst at a temperature of 1120°C in presence of pure O_2 . Evolved gases were passed through a reduction reactor containing reduced copper granules at a temperature of 850°C to convert all NO_x compounds to N_2 followed by a moisture trap filled with Sicapent (V_2O_5). Dry gas streams of N_2 , CO_2 , and SO_2 were carried by dry Helium gas further towards IRMS. N_2 stream was allowed to go into the analyzer of IRMS for its

stable mass-spectrometric analysis without any inhibition, while CO₂ and SO₂ streams were held on specially designed adsorption columns to ensure sequential mass-spectrometric analysis of these gas streams. The detailed methodology adopted for isotopic analysis are published elsewhere (Agnihotri et al., 2014). Mass-spectrometric current generated by sample gas streams were calibrated to measured mass concentrations of TC, TN, and TS. The C, N, and S isotopic anomalies were expressed in their standard delta notation using following equation 1.

$$\Delta = [(R_{\text{sample}} / R_{\text{standard}}) - 1] \times 1000 \text{---(1)}$$

Where, R= ¹³C/¹²C, ¹⁵N/¹⁴N, ³⁴S/³²S

Internationally accepted standards for expressing $\Delta^{13}\text{C}$ values are Vienna-Pee Dee Belemnite (V-PDB), while atmospheric N₂ is used for expressing $\Delta^{15}\text{N}$ values. For Sisotopic anomaly Vienna-Canyon Diablo Troilite (V-CDT) is used. Δ values are expressed in per thousand (commonly known as ‘per mil’ denoted by ‰).

For ascertaining the accuracy and precision of all the stable isotopic measurements, a suite of *in-house* and *international* IAEA standards was used. The instrument is mainly calibrated by four-point calibrations using an international standard i.e. e-Amino-n-Caproic acid [C₆H₁₅NO₂] generally known as ACA for $\Delta^{13}\text{C}$ and $\Delta^{15}\text{N}$ having standard amount between 0.5 and 4 nmol with known stable carbon and nitrogen isotopic composition as –25.3‰ and 4.6 respectively. The $\Delta^{34}\text{S}$ values were constrained by standard IAEA-S-2 and in-house sulphanilamide with a known isotopic value 22.7±0.7 and 1.23 ±0.12 ‰ respectively (Agnihotri et al., 2014; Sawlani et al., 2019). Overall analytical uncertainties in the measurement of $\Delta^{13}\text{C}$, $\Delta^{15}\text{N}$ were within 0.2‰, and within 0.3‰ for $\Delta^{34}\text{S}$.

2.3 Backward trajectory analysis of air mass

2.3.1 Trajectory Data

To identify the route of air mass blowing over New Delhi at 500 metre above ground level (MAGL), 72-hour back-trajectories were obtained from the web version of the Hybrid Single-Particle Lagrangian Integrated Trajectory- 4 (HYSPLIT) model, which utilizes NCEP/NCAR reanalysis meteorological database (Stein et al., 2015). Daily meteorological data were acquired from the global data assimilation system (GDAS) provided by NCEP (source:<http://www.arl.noaa.gov/ready/hysplit4.html>). Results of cluster analysis of winds (at 500 MAGL) were used to understand the impacts of long range transport of particles and pollutants over the sampling site (Hsu et al., 2003a; McGowan and Clark, 2008), as mixing layer of tropospheric air at this height is recommended to be useful (Gao et al., 1995).

2.3.2 Trajectory clustering

We carried out multivariate statistical analysis of backward winds, a technique that divides the trajectory data into distinct clusters. TriStat software (version:1.2.2.6) provides two clustering methods i.e. angle distance and euclidean distance. The objective of the analysis is to identify the direction from where the air mass arrives at the site, for which the method of angle distance can be used, which is defined using the law of cosines (Sirois and Bottenheim, 1995). The angle distance between two air mass backward trajectories was given by equation 2.

$$d_{12} = \frac{1}{n} \sum_{i=1}^n \frac{1}{\cos} \left(0.5 \frac{(A_i + B_i + C_i)}{\sqrt{A_i B_i}} \right) \quad \dots \quad (2)$$

Where,

$$A_i = (X_1(i) - X_0)^2 + (Y_1(i) - Y_0)^2,$$

$$B_i = (X_2(i) - X_0)^2 + (Y_2(i) - Y_0)^2,$$

$$C_i = (X_2(i) - X_1)^2 + (Y_2(i) - Y_1)^2,$$

The variables X_0 and Y_0 are the position of the studied site $X_1(i)$, $Y_1(i)$, and $X_2(i)$, $Y_2(i)$ are coordinates of i segment for trajectories 1 and 2. For characterizing significant seasonal differences in air mass transportation influencing ambient PM_{2.5} aerosol properties, all three major seasons (post monsoon, winter, and summer) were analyzed.

2.3.3 Concentrated Weighted Trajectories (CWT) method

The CWT model is used to estimate the potential impact of the regional sources over the receptor site to calculate the trajectory weighted concentrations (Hsu et al., 2003b; Liu et al., 2013; Wang et al., 2006, 2009). In addition to providing information on the spatial distribution of the sources, it gives information on the relative significance of different potential source regions (Liu et al., 2013). The CWT concentrations can be generated using Trajstat algorithm which covers the entire geographic region by the trajectories divided into an array of grid cells. Then each grid cell is assigned a weighted concentration value at the receptor site by averaging the pollutants' concentration that has associated trajectories crossing that grid cell (Hsu et al., 2003b) as given in equation 3 below:

$$C_{ij} = \frac{1}{\sum_{l=1}^M \tau_{ijl}} \sum_{l=1}^M Cl \tau_{ijl} \quad \dots \quad (3)$$

where C_{ij} is the average weighted concentration of PM_{2.5} in the grid cell (i, j) , l is the index of the trajectory, M is the total number of trajectories, Cl is the concentration observed at the sampling location (receptor site) on the arrival of trajectory l , and τ_{ijl} is the residence time (time spent) of trajectory l in the grid cell (i, j) . A high value for C_{ij} implies that air parcels traveling over the grid cell (i, j) would be, on average, associated with high concentrations at the receptor site. In this study, CWT algorithm was investigated independently for PM_{2.5} to distinguish the origin of air masses influencing PM size distribution over New Delhi in different seasons. The geographical domain was

divided into grid cells of 0.5° by 0.5° .

3. Results

3.1 Sky conditions over New Delhi and NCR from satellite imagery

Figs.1A&B show maps of India and Delhi state respectively, with state and district boundaries. To understand the seasonal variations of different pollution sources over sampling site, season-wise composite fire-count data (of north India) and typical day satellite imageries showing lower atmospheric transparency of sky over New Delhi and NCR region is presented in Figs.1C-H. Daily images obtained from Moderate Resolution Imaging Spectro-radiometer (MODIS) Aqua satellite were processed for obtaining representative (comPOSITE) fire-count images for post-monsoon, winter and spring-summer seasons. Red dots in Figs 1C-H indicate fire-counts. It can be observed that the fire-count intensity was most intense in post-monsoon season as compared to that of during spring-summer and winter seasons and this is associated with the burning of crop-residue left after harvesting season in north India. This is an annual activity dominating in the October-November months of every year that was followed by frequent haze (SMOG) episodes over Delhi stretching over entire IGP (Sawlani et al., 2019). For instance, Fig. 1D shows a MODIS image of the north India for a randomly chosen day of 12th November, 2014 showing the impacts of a hazy episode occurred following 10th November, 2014. It is evident that a thick smoke layer was present over the region which can be well corroborated by recorded increased PM_{2.5} loading in November 2014 (Fig. 2A). In contrast to post-monsoon and winter seasons, spring-summer months of north India generally experience cleaner skies. Fig. 1H represents a clear and sunny day image of 9th April 2015, which can be used to gauge the difference between polluted and non-polluted skies of north India.

3.2 PM_{2.5}, TC, TN and TS concentrations and their stable isotopic values

We evaluated season-wise statistics of all measured chemical and isotopic data in tandem with major meteorological parameters (averages are given with the standard deviations depicting the range of values observed) and major relevant gaseous concentrations (24 hour averaged) for a relative assessment purpose (Table 1). PM_{2.5} concentrations varied in the range between 43.9 to 453.7 $\mu\text{g m}^{-3}$ with an average value of $184.4 \pm 87.5 \mu\text{g m}^{-3}$, which is about three fold higher than the recommended safety PM_{2.5} levels ($\sim 60 \mu\text{g.m}^{-3}$) set by the CPCB as National Ambient Air Quality Standards (NAAQS) for the healthy human respiratory system (Xing et al., 2016).

Measured mass concentration of PM_{2.5} along with their TC, TN, and TS content data for aerosol samples collected between September 2014 to May 2015 are shown in Fig. 2. Stable isotopic data of all three major components i.e. $\square^{13}\text{C}$, $\square^{15}\text{N}$ and $\square^{34}\text{S}$ are also plotted. PM_{2.5} and TC concentrations show enhancement right after the post-monsoon season in north India, which coincides with the harvesting period for Kharif crop. The entire late post-monsoon and winter months experience enhanced PM_{2.5} loadings. Peak winter months (December and January) clearly show enhanced TN and TS concentrations, thereby appear to be massively contributing in building up ambient PM_{2.5} pollution.

During the entire study period, maximum PM_{2.5} concentrations were found during the winter months with an average value of $220 \pm 93 \mu\text{g m}^{-3}$. Winter averages of PM_{2.5} concentrations were found to be similar to those of post-monsoon months with average value of $194 \pm 99 \mu\text{g m}^{-3}$. Spring-summer months (March to May) showed relatively lower values of PM_{2.5}, averaging $136 \pm 55 \mu\text{g m}^{-3}$ (Table 1). Thus, PM_{2.5} levels over New Delhi even for the spring-summer season were found to be around two fold higher than recommended safe levels for ‘good’ air-quality.

Aerosol TC concentrations varied between 22.6 to 228.6 $\mu\text{g m}^{-3}$ with an average value of $87.9 \pm 44.3 \mu\text{g m}^{-3}$. Maximum TC concentrations were observed during winter season with an average value of

$100\pm42.6 \text{ } \mu\text{g m}^{-3}$ and minimum in spring-summer season with average value of $61.4\pm18.8 \text{ } \mu\text{g m}^{-3}$ (Fig. 2B, Table 1). $\square^{13}\text{C}_{\text{PM}2.5}$ values varied between -29.6 to $-20.9 \text{ } \text{\textperthousand}$ with an average value of $-25.4\pm1.5 \text{ } \text{\textperthousand}$. During the post-monsoon, winter and summer season, the ranges observed in $\square^{13}\text{C}_{\text{PM}2.5}$ values were $-26.0\pm0.8 \text{ } \text{\textperthousand}$, $-25.5\pm1.2 \text{ } \text{\textperthousand}$, and $-24.9\pm1.9 \text{ } \text{\textperthousand}$ respectively (Fig. 2B, Table1). Aerosol TN concentrations varied between 1.4 to $51.3 \text{ } \mu\text{g m}^{-3}$ with an average value of $15.4\pm13 \text{ } \mu\text{g m}^{-3}$ (Fig. 2C, Table1). During the study period, maximum TN contents were observed during winter season with an average value $24\pm13.8 \text{ } \mu\text{g m}^{-3}$. Average TN concentrations for post-monsoon months were two fold lower with an average value of $13\pm7.3 \text{ } \mu\text{g m}^{-3}$. Spring-summer months showed a further two fold reduction with average TN concentrations as $4.5\pm1.4 \text{ } \mu\text{g m}^{-3}$ (Fig. 2C, Table1). $\square^{15}\text{N}_{\text{PM}2.5}$ showed average value of $9.0\pm3.9 \text{ } \text{\textperthousand}$ with a large range of variability between 0.4 and 19.4 (Fig. 2C). $\square^{15}\text{N}_{\text{PM}2.5}$ values of spring-summer months were about $\sim 5 \text{ } \text{\textperthousand}$ higher (averaging $12.3\pm4.6 \text{ } \text{\textperthousand}$) compared to those during post-monsoon and winter months ($7.7\pm4.1 \text{ } \text{\textperthousand}$, $7.3\pm6.6 \text{ } \text{\textperthousand}$ respectively; Fig. 2C, Table1).

Aerosol TS concentrations varied between 0.2 to $63.5 \text{ } \mu\text{g m}^{-3}$ with an average of $13.1\pm13.1 \text{ } \mu\text{g m}^{-3}$ (Fig. 2D). Maximum TS contents were observed during winter months with an average value of $13.5\pm11.6 \text{ } \mu\text{g m}^{-3}$ and minimum in spring-summer season i.e. $4.0\pm3.6 \text{ } \mu\text{g m}^{-3}$ (Fig. 2D, Table1). $\square^{34}\text{S}_{\text{PM}2.5}$ values also showed two conspicuous peaks between October-November and November-Decemeber (Fig. 2D). Average $\square^{34}\text{S}_{\text{PM}2.5}$ values during post-monsoon, winter and summer seasons were found to be varying in overlapping ranges of $3.5\pm2.0 \text{ } \text{\textperthousand}$, $3.1\pm1.1 \text{ } \text{\textperthousand}$, and $3.8\pm0.8 \text{ } \text{\textperthousand}$ respectively (Fig. 2D, Table1).

Fig. 3A shows monthly average values of $\text{PM}_{2.5}$ and TC concentrations plotted with monthly mean values of ambient relative humidity and temperature data. Likewise, aerosols' monthly mean concentrations of TN and TS components were plotted with lower-atmospheric NH_3 , NO_x and SO_2

concentrations (Fig. 3B). It can be seen that ambient PM_{2.5} levels over New Delhi demonstrate a typical negative correlation with ambient temperatures and an overall positive correlation (but in a non-linear fashion) with relative humidity (Fig. 3A). Ambient NO_x and NH₃ concentrations showed linear increases from September and October to December and January respectively (Fig. 3B). These trends reveal dominant roles of these gaseous N species in producing particulate TN component of PM_{2.5}. Atmospheric SO₂ concentrations, in contrast, remain similar (within overlapping ranges) till December and show significant increase from December to April (Fig. 3B). Ambient NH₃ levels showed a steep fall after January but NO_x levels remained, by and large, similar after peak winter month of January (Fig. 3B). Hence there are clearly different dissipating pathways for the mentioned two N species.

We decided to probe further TN and $\square^{15}\text{N}_{\text{PM}2.5}$ variabilities in relation to same day recorded ambient NH₃ and NO_x data (Fig. 4). Aerosol TN contents and ambient NH₃ concentrations showed a significant positive correlation (Fig. 4A; $r=0.79$, $p=0.001$) as anticipated (Pavuluri et al., 2010). It is because elevated NH₃ levels have been reported to produce elevated NH₄⁺ ions which react with ambient SO₄⁻² (to produce (NH₄)₂SO₄ and NH₄HSO₄) suggesting that the atmospheric NH₃ majorly influences aerosol (particulate) N mass (Meng et al., 2018). $\square^{15}\text{N}_{\text{PM}2.5}$ values also show a noteworthy positive correlation ($r=0.82$; $p=0.001$) with ambient NH₃ concentrations during peak winter period (December, January; Fig. 4B). Earlier studies from south India (e.g. Pavuluri et al., 2010) also have revealed that bulk $\square^{15}\text{N}$ values of aerosol particles mainly represent isotopic values of aerosols' ammonium (NH₄⁺) fraction. Ambient NO_x, on the other hand, shows enhanced concentrations during late post-monsoon-early-winter and spring-summer periods, suggesting their relatively less important role in building up of ambient PM_{2.5} in the lower atmosphere of New Delhi. It may be due to

continuous production and destruction of aerosol N oxides. Aforementioned relationships between ambient NH₃, aerosol TN contents and $\square^{15}\text{N}_{\text{PM}2.5}$ indicate that bulk of aerosol particulate N could be resulting from atmospheric NH₃ emissions originating from agricultural soils of neighbouring states (Punjab-Haryana). Volatilization loss of N as NH₃ from North India's rice-wheat cropping system was recorded in the range 10–70 kg N ha⁻¹ depending on the fertilizer application dose (Banerjee et al., 2002, Pathak et al., 2006, Prashad et al., 2006). It should be noted that global ammonia emission has almost doubled since preindustrial times, mainly because of agricultural intensification (Galloway et al., 2003). Cluster analysis of wind trajectories and concentration weighted trajectories for New Delhi (Fig. 8; discussed later) corroborate aforementioned contention.

To infer about probable sources of aerosol C, N and S components during post-monsoon, winter and spring-summer months, we show season-wise and box-whiskers of $\square^{13}\text{C}_{\text{PM}2.5}$, $\square^{15}\text{N}_{\text{PM}2.5}$ and $\square^{34}\text{S}_{\text{PM}2.5}$ values along with source (end-member) isotopic data. Source isotopic composition data have been adopted from various publications mentioned on the caption of Fig. 5. It can be seen that C component of ambient PM_{2.5} particles appear to be largely contributed by biomass burning and fossil-fuel (diesel) combustion related emissions during all three seasons (Fig. 5A). Aerosol N compounds appear to be largely contributed by emissions from coal- and fossil-fuel combustions during both post-monsoon and winter months, while emissions from biomass and biofuel burning appear to contribute N component of ambient PM_{2.5} particles during spring-summer months (Fig. 5B). It is noteworthy that aerosol S component was found to be largely contributed by coal- and fossil-fuel combustions, road-dust and possibly by biogenic S emissions (Fig. 5C).

Fig. 6 focuses on inter-relationships between aerosol chemical (and isotopic) characteristics with ambient air-quality & meteorological parameters. Synergies between aerosol chemistry and ambient meteorology are expected to play very important roles in PM pollution (Baklanov et al., 2018). In

view of this, we investigated monthly variability in ambient PM_{2.5}, TC, TN and TS data in relation to monthly means of surface solar radiation (watt. m⁻²), air-visibility, relative humidity and temperature data (Fig. 6). PM_{2.5} and its TC+TN+TS contents clearly demonstrate that their quanta adversely impact surface solar radiation and air-visibility values (Fig. 6A). Air-visibility is an important parameter in determining the air-quality index (AQI) in New Delhi (Singh and Dey, 2012). It is worth mentioning here that solar radiation (watt. m⁻²) data for all sampling days were averaged between noon 12:00 hrs to 14:00 hrs. Fig. 6A reveals the dominant role of PM_{2.5} and their carbonaceous and sulphur components in blocking and scattering the solar radiation over New Delhi. Similar to the case for New Delhi, air-visibility in China also has shown considerable reductions in recent years which has been attributed to the increase of the atmospheric concentrations of fine particulate matter (PM_{2.5}) (Wu et al. 2012). Fig. 6B shows monthly ranges of □¹⁵N_{PM2.5} values plotted along with contemporaneous surface solar radiation and air-visibility. Notably □¹⁵N_{PM2.5} values appear to shift toward lower numbers (toward 0.0‰) for November, December and January, when air-quality parameters tend to approach to their worst degraded values. This could be understood as lower □¹⁵N_{PM2.5} values mainly originate from NH₃ emissions (gaseous NH₃ conversion to particulate NH₄⁺) and NO_x emissions emanating from vehicular emissions (diesel- petrol combustion). Fig. 6C shows monthly ranges of □³⁴S_{PM2.5} values plotted along with monthly ranges of ambient relative humidity and temperatures. Aerosol □³⁴S values vary in relatively wider and overlapping ranges during post-monsoon to peak winter months (December and January) and do not show any clear relationship with ambient relative humidity and temperatures, but from January onwards there appears to be a systematic enrichment in □³⁴S_{PM2.5} values. During this period ambient temperatures also show a step-wise enhancement along with a systematic (step-wise) decline in relative humidity (Fig. 6C). Hence, in case of aerosols' S proportion too, lowest □³⁴S_{PM2.5} values were found during peak winter month

(January) that is known for poorest air-visibility (and air-quality) in NCR region. Most plausible sources for aerosol S during peak winter are from burning of coal and dung-cake fuels and biogenic S emissions (Fig. 5C). Hence, both N and S contents as well as their isotopic values appear to be modulated by specific sources' contributions and meteorological parameters.

Prompted by aforesaid observations, we decided to investigate inter-relationships between aerosol-chemistry and ambient meteorology more intrusively and noted several statistically significant relationships as shown in Fig. 1S (Supplementary material¹). Aerosol TC concentrations showed significant anti-correlations with ambient temperature, air-visibility and surface solar radiation data (Fig. 1S A-C). These inverse relationships get strengthened even more for post-monsoon and winter months. No such significant correlations, however, were observed between $\square^{13}\text{C}_{\text{PM}2.5}$ values and any of aforementioned meteorological parameters (cross-plots therefore not shown), indicating minimal changes in aerosols' carbon inventory. Aerosol TN contents revealed strikingly significant inverse-relationships with ambient temperature, air-visibility, surface solar radiation data and positive correlation with ambient relative humidity (Fig. 1S D-G). This could be understood in terms of destruction of aerosols' particulate N species in the presence of solar radiation and rising ambient temperatures. Our contention gets corroboration from N isotopic data, as $\square^{15}\text{N}_{\text{PM}2.5}$ values did not show any significant correlation with relative humidity (cross-plot not shown) but showed noteworthy significant positive correlations with ambient temperature and surface solar radiation (Fig. 1S H-I). It is important to note that both TS concentrations and $\square^{34}\text{S}$ values showed strong non-linear (as well as linear) relationships with major meteorological parameters. For instance, TS concentrations showed cubic (inverse) relationships with air-visibility and ambient temperature. TS concentrations showed a positive cubic relationship with relative humidity (Fig. 1S J-L). Aerosol

$\square^{34}\text{S}$ values, in contrast, showed significant linear positive relationships with air-visibility and ambient temperature and a significant anti-correlation with relative humidity data (Fig. 1S M-O). Apparently, high loading of particulate S in winter season appears to be manifested by sharp increase in relative humidity and decrease in ambient temperatures. Aforementioned real time relationships could be further investigated in laboratory controlled experiments for better understanding of involved mechanism.

Strong positive correlation was observed between aerosol TN and TS concentrations for winter months, indicating that the N and S gaseous species of aerosol particulate phase are formed via gas to particle conversions under ‘conducive’ meteorological conditions prevailing over New Delhi leading to amplifications of $\text{PM}_{2.5}$ pollution from ‘bad’ ($\text{PM}_{2.5} \sim 100\text{-}150 \mu\text{g.m}^{-3}$) to ‘severe’ ($\text{PM}_{2.5} \geq 300 \mu\text{g.m}^{-3}$) level.

3.3 Atmospheric haziness and role of ammonia

In many urban centres of China (e.g. Beijing), high production of secondary inorganic aerosols (SIAs) relative to secondary organic aerosols (SOA) have been observed during intense atmospheric haze episodes (An et al., 2019, Wang et al., 2019). Three dimensional cross-plots shown in Fig.7 clearly reveal how enhanced ambient NH_3 gets converted into particulate TN fraction (of $\text{PM}_{2.5}$ aerosols) under enhanced relative humidity and declined temperatures that eventually result in atmospheric haziness. It can be seen that when NH_3 levels exceed concentrations of $>\sim 300 \mu\text{g m}^{-3}$ (Fig. 7B) and meteorology is favourable *i.e.* enhanced humid condition ($>70\text{-}80\%$; Fig. 7A) with reduced ambient temperatures ($\leq 15\text{-}20^\circ\text{C}$), there is a high probability of encountering poor air-visibility and atmospheric haziness in New Delhi and NCR region.

3.4 Cluster and Concentration weighted (wind-) trajectory analysis for New Delhi

To study the potential sources and atmospheric circulation pathways, cluster analysis, and CWT methods were executed for each season and the results are shown in Fig.8. For best representation of air mass classifications, an attempt was made to use six clusters (C1 to C6) for each season (Fig.8A-C). Cluster analysis reveals that during the post monsoon season (Fig. 8A), cluster C1 originating from southwest Arabian sea constitute 22% of trajectories, C3, C4 and C5 clusters contribute maximum 64% and originate from northwest of Pakistan and neighbouring states of Punjab and Haryana while the short re-circulating cluster C2 initiate from the east of Delhi and contributes 14 % of trajectory clusters. Similarly in winter season (Fig. 8B), which is mainly affected by sub-regional and regional pollution sources, long clusters C3 and C6 contribute highest with 58% and arise from northwest, C5 from southwest i.e., from Pakistan through Rajasthan that adds 8% trajectories, C4 from southeast Uttar Pradesh region which adds 10% trajectories however, shorter re-circulating clusters C1 and C2 initiate from north west and northeast. During the summer season which is dominated by westerly flows (Fig. 8C), long cluster C5 coming from the Sahara Desert contribute to 6% of the trajectories, C3 originating from the Arabian Sea contribute 6% to the trajectories, C6 and C4 hailing from north west Pakistan-Afghanistan region dominate with 42 % and C2 originating from south east in Uttar Pradesh adds 17%. The shorter re-circulating trajectory cluster C1 around Delhi area constitute second largest contribution with 29% to the trajectories.

Furthermore, the results for [PM_{2.5}] derived by the CWT method are presented in Fig. 8D-F. The regions with high intensity of red colour correspond to the major contributing sources associated with the high PM_{2.5} values. The post monsoon season analysis reveals that high CWT values corresponding to origin of air mass was distributed amongst Pakistan, Punjab, Haryana and Western Uttar Pradesh. It demonstrates that the contribution from long-range transport and sources outside of

New Delhi were significant in post monsoon season which influence PM_{2.5} levels in New Delhi. In contrast, summer has most CWT values lying between 20 and 80 $\mu\text{g m}^{-3}$ which indicate that there are no major important potential source areas. The only major contribution is from the long range transport from Sahara and Thar Desert of Rajasthan (Fig. 8F). The winter analysis demonstrates the CWT concentration gradients represented by red hotspots, with maximum potential contribution from sub-regional and regional sources comprising of neighbouring states of Punjab, Haryana, and Uttar Pradesh (Fig. 8E).

4. Discussion

New Delhi has emerged as a globally recognized hotspot of PM_{2.5} pollution categorizing from severe ($\text{PM}_{2.5} \geq 300 \mu\text{g.m}^{-3}$) to critical level ($\text{PM}_{2.5} \geq 400 \mu\text{g.m}^{-3}$) air pollution events just after post-monsoon (late-October to December) inducing acute disruptions in air and land traffic besides affecting the normal life of majority of human populations living in the national capital territory. From our study, it is evident that aerosols' CNS contents considerably inhibit significant proportions of surface solar radiation and reduce air-visibility with a combined effect on atmospheric haziness in New Delhi and NCR.

Average mass concentrations of TC during post-monsoon, winter and spring-summer months accounted for ~50.4%, 45.5% and 45.3% of the average mass concentration of PM_{2.5} in New Delhi. These values could be compared with average TC contribution to ambient PM_{2.5} in Beijing, Tianjin, and Langfang (Chinese cities) varying as 30.5%, 24.8%, and 49% (sampled between November and December 2016) (Qi et al., 2018). Comparable and high aerosol TC concentrations were observed during both post-monsoon and winter months with overlapping $\square^{13}\text{C}$ values (Fig. 2B). This shows that the probable sources of TC in ambient PM_{2.5} particles could be emissions from combustion of agricultural crop-residue burning (Sawlani et al., 2019; Takigawa et al., 2020), vehicular emissions

(burning of petrol & diesel) and coal burning (for power generation). Aerosol $\square^{13}\text{C}$ values during post-monsoon varied in a range between -28.5 to $-24.5\text{\textperthousand}$ (Table 1). The observed range suggests that these aerosol $\square^{13}\text{C}$ values could be manifested by three major contributors (i) emissions from burning of C3 type biomass typified by $\square^{13}\text{C}$ values $\sim -28 \pm 1.0\text{\textperthousand}$, diesel combustions characterized by $\square^{13}\text{C}$ values $\sim -26 \pm 0.5\text{\textperthousand}$ and coal burning emissions characterized by $\square^{13}\text{C}$ values $\sim -22 \pm 1.0\text{\textperthousand}$ (see Fig. 5A). It should be noted that $\square^{13}\text{C}$ values would be $-13 \pm 4\text{\textperthousand}$ if emissions from C4 type biomass burning are prevalent (Boutton et al., 1998). Aerosol $\square^{13}\text{C}$ values showed an abrupt rise and fall during spring-summer months (Fig. 2B), averaging $-24.9 \pm 1.4\text{\textperthousand}$ (range between -29.5 to $-20.9\text{\textperthousand}$) (Table 1). Average $\square^{13}\text{C}_{\text{PM}2.5}$ values for New Delhi are similar as have been noted for other mega cities of the world such as Tokyo, and Mexico city (Anclet et al., 2011; Dai et al., 2015; López-Veneroni, 2009; Widory, 2006). The abrupt rise and fall during spring-summer $\square^{13}\text{C}_{\text{PM}2.5}$ may be attributed to the inventory of dust carrying carbonate-carbon from the Thar Desert area. Similar $\square^{13}\text{C}_{\text{PM}2.5}$ values i.e. values between $-22\text{\textperthousand}$ to $-25\text{\textperthousand}$ are reported for Gosan site in Jeju Island (South Korea) (Kawamura et al., 2004) and $-21 \pm 0.2\text{\textperthousand}$ (López-Veneroni, 2009). This interpretation is well supported by summer season air-mass backward trajectory (Fig. 8C). Clustered and concentration weighted wind trajectories over New Delhi clearly showed dominance of crop-residue burning emissions' contributing to PM_{2.5} pollution in atmosphere over New Delhi during late post-monsoon season (Figs. 1C-D, 8A, D).

Winter months in New Delhi, however, appear to be dominated by enhanced particulate phase conversions of N and S species via gas to particle conversions taking place amidst declined ambient temperatures and enhanced relative humidity (Fig. 2C,D, Figs. 3-4). Both of these meteorological changes are known to enhance atmospheric haziness via variety of chemical reactions (An et al., 2019; Aggarwal et al., 2013; Pavuluri et al., 2010; Plautz, 2018; Sawlani et al., 2019; Wang et al.,

2019; Zhang and Samet, 2015). Our study tends to be in line with earlier observation that noted the SIAs play a major role in creating haziness episodes (Plautz, 2018; Sun et al., 2014). SIAs get formed when atmospheric ammonia (NH_3) reacts with acidic compounds such as sulphuric acid (H_2SO_4) and nitric acid (HNO_3) to form particulate ammonium sulphate and nitrate [$(\text{NH}_4)_2\text{SO}_4$ and NH_4NO_3] (Griffith et al., 2015; Plautz, 2018). Formation of ammonium (NH_4^+) aerosols is favoured under enhanced relative humidity (70-90%) (Pan et al., 2016).

Average $\square^{15}\text{N}_{\text{PM}2.5}$ values for both post-monsoon and winter months are similar and closely overlap, whereas $\square^{15}\text{N}_{\text{PM}2.5}$ values for spring-summer season were relatively enriched. Fig. 5B clearly reveals that likely sources of aerosol N during post-monsoon and winter times are coal and fossil fuel combustions. However, relatively enriched $\square^{15}\text{N}_{\text{PM}2.5}$ values of spring-summer months could be likely due to altered sources such as emissions from biomass burning (Fig. 5B) and secondary processing of particles leading to isotopic enrichment of residual N under enhanced (warmer) temperatures and abundant surface solar radiation. $\square^{15}\text{N}_{\text{PM}2.5}$ values of post-monsoon and winter months are comparable with the values reported by Widory (2007) and Sawlani et al. (2019) for Paris and New Delhi respectively. Average $\square^{15}\text{N}$ values for major combustion sources are: diesel ($4.6 \pm 0.8 \text{‰}$), natural gas ($7.7 \pm 5.9 \text{‰}$), unleaded gasoline ($\sim 4.6 \text{‰}$), waste incinerators (5.5 to 8 ‰), cattle dung-cake ($5.1 \pm 1.4 \text{‰}$), Coal ($8.6 \pm 0.3 \text{‰}$), C3 biomass ($5.9 \pm 4.2 \text{‰}$), Dust ($5.7 \pm 0.3 \text{‰}$) (Sawlani et al., 2019; Widory, 2007). As has been said earlier, depleted $\square^{15}\text{N}_{\text{PM}2.5}$ values during winter and post-monsoon seasons possibly indicate dominance of secondary formed NH_4^+ (from NH_3 emissions originating from agricultural soils) (Chang et al., 2019; David Felix et al., 2013; Pan et al., 2016). High aerosol loading of N could be attributed to the enhanced agricultural usage of nitrogenous fertilizers on fields (Liu et al., 2013). New Delhi and NCR are surrounded by agricultural rich states and, for good productivity, farmers use excess amounts of N-fertilizers. After assimilation of

fertilizers, remaining fertilizers get converted into ammonia by the process of denitrification (B. et al., 2002; Datta et al., 2012; Pathak et al., 2006; Sharma et al., 2007). NH₃ emissions are generally characterized by isotopically depleted $\Delta^{15}\text{N}$ values (~ -5 to $-8\text{\textperthousand}$; Jickells et al., 2003). Meteorological impacts were noticeable as highest atmospheric NH₃ concentrations were found over New Delhi under enhanced relative humidity and declined temperature (Fig.7). These additional factors can induce prolong episodes of atmospheric haziness (Pan et al., 2016b; Plautz, 2018). Even though this study clearly brings out importance of atmospheric NH₃ and its particulate conversion (into NH₄⁺) resulting in atmospheric hazy days over New Delhi, it must be noted that sources of this atmospheric inorganic pollutants are not well constrained regionally. Atmospheric NH₃ is not included in the emission control policies for major populated centres of India or China (Pan et al., 2016). Relative emission strengths of NH₃ sources from agricultural sector versus transport sector remains to be quantified. It was important to note that aerosol $\Delta^{15}\text{N}$ values showed positive correlations with ambient temperature and surface solar radiation data (Fig. 1S H-I) suggesting destructions of N particulate phase species and progressively enriching residual pool of N (of ambient PM_{2.5} particles) as temperature rise and solar radiation becomes available. Hence aforementioned meteorological factors appear to play vital roles to have clearer and cleaner skies over New Delhi and NCR.

Like the case for TN, TS concentrations of ambient PM_{2.5} particles were highest for winter months (Fig.2D). A significant positive correlation ($r=0.80$) was noted between TS and TN concentrations for winter season [unlike for post-monsoon ($r=0.3$) and springs-summer months ($r=0.03$)]. This observation clearly reveals the predominant role of N and S particulate species in enhancing PM_{2.5} pollution in New Delhi. (NH₄)₂SO₄ and NH₄HSO₄ could be likely compounds produced via gas to particulate conversion reactions. Aerosol sulphate component is known to play an important role in

the regional radiation budget and has a cooling effect for climate change (Charlson et al., 1990; Kiehl et al., 2000; Kirkevåg et al., 1999). Norman et al. (1999) reported aerosol $\square^{34}\text{S}$ values near to 5‰ for places which are intensely affected by the urban pollution with predominance of fossil fuel combustion. Similar values were found by us also in our previous studies for aerosols over Goa and New Delhi (Agnihotri, 2015; Sawlani et al., 2019). Stable isotope composition of S in the atmosphere is quite variable. Typically, atmospheric particulate S could be of marine biogenic origin (with $\square^{34}\text{S}$ values $\sim +15\text{--}17\text{\textperthousand}$), sea-salt spray ($\square^{34}\text{S}$ values $\sim +21.2\text{\textperthousand}$), or produced by oxidation of local H_2S (into SO_2) emitting during decay of organic matter (Han et al., 2015; Jamieson and Wadleigh, 2000; Norman et al., 1999; Romero, 2003). Average $\square^{34}\text{S}_{\text{PM}2.5}$ values of ambient $\text{PM}_{2.5}$ size particles for all the months (September 2014 to May 2015) show values between $\sim 3\text{--}4\text{\textperthousand}$, ruling out significance of sulphates emanating from marine sources for the land-locked New Delhi region. The measured $\square^{34}\text{S}$ range overlaps with range reported by Neumann and Forrest (1991). They reported the $\square^{34}\text{S}$ isotopic composition of fuel oil and coal from different places which were ranging from $-10\text{\textperthousand}$ to $+16\text{\textperthousand}$ with an average of $4\pm 5\text{\textperthousand}$. Observed $\square^{34}\text{S}_{\text{PM}2.5}$ values could be a resultant of contribution by a variety of sources such as emissions from diesel ($2.1\pm 1.8\text{\textperthousand}$), coal (3.1 ± 0.4 to $8.6\pm 0.3\text{\textperthousand}$), cattle dung-cake ($\sim 4.4\text{\textperthousand}$), and soil-dust ($2.0\pm 0.4\text{\textperthousand}$) (Sawlani et al., 2019). Fig. 5C clearly reveals possibility of biogenic S emissions and their gaseous to particle-phase conversions in ambient atmospheres over New Delhi, besides emissions from coal and dung-cake combustions.

Notably both TS and $\square^{34}\text{S}_{\text{PM}2.5}$ values demonstrate statistically significant correlations with majority of meteorological and air-quality parameters (Fig. 1SJ-O). This could be seen as a result of variation in S isotope fractionation influenced by meteorological parameters (Han et al., 2016). These meteorological parameters' influences on aerosol $\square^{34}\text{S}_{\text{PM}2.5}$ values indicate considerable secondary processing of fine particles. Besides meteorological effects, recent studies have shown that oxidation

of SO_2 by OH radicals, H_2O_2 and transition metal ion catalysis (TMI) also play an important role in fractionating $\square^{34}\text{S}$ values (Harris et al., 2012). Lower aerosol $\square^{34}\text{S}$ values during poor air-visibility periods (Fig. 6C) indicates removal of soluble S in moist conditions via heterogeneous oxidation pathways in winter months (Saltzman et al., 1983). Oxidation of SO_2 gas released from sulphate-rich aerosol particles leads to change in the isotopic composition of the primary bound sulphur (Krouse et al., 1991; Nielsen, 1974). It is important to note that a conspicuous shift towards lower aerosol $\delta^{34}\text{S}$ values was seen for severe post-Diwali SMOG phase (31 October to 7th November, 2016) over New Delhi (Sawlani et al., 2019). Wang et al. (2016) have reported that low photochemical activity during the hazy skies enhances atmospheric SO_4^{2-} levels. Alternatively, particulate sulphate oxidation can be catalyzed by available free metal ions in the lower atmosphere emanating from various heterogeneous sources (such as cracker bursting during Diwali festival celebrated in north India during late October-November) (Sawlani et al., 2019). These processes might enhance atmospheric haziness. $\delta^{34}\text{S}_{\text{PM}2.5}$ data for New Delhi (averaging $3.6 \pm 1.2\text{\textperthousand}$; Table 1) could be seen as distinctly different from $\delta^{34}\text{S}$ data of marine or biomass burning emissions data (Fig. 5C). However, it is important to note that aerosol data for urban locations surrounded by marine region such as Goa and Port Blair (Andaman, India) also ranged from $1.25 \pm 1.03\text{\textperthousand}$ (Agnihotri, 2015; Rastogi et al., 2020) indicating dominance of local scale emissions and secondary processing of aerosol sulfur.

Conclusions

- 1- Concentration of $\text{PM}_{2.5}$ size aerosols was found to be considerably higher (by a factor of 2-5) with respect to the maximum permissible values set by NAAQS in Delhi during the entire non-monsoon proportion of the year 2014-15.
- 2- Maximum $\text{PM}_{2.5}$ concentrations were observed during winter months. Significant enhancement in both N and S mass concentrations during peak winter indicated that N and S are the major species responsible for higher $\text{PM}_{2.5}$ levels in New Delhi and NCR.
- 3- $\square^{13}\text{C}_{\text{PM}2.5}$ values for post-monsoon months indicate C3 plants' biomass burning in northwest

IGP region as major source. This is additionally contributed by the mixing of other anthropogenic emissions such as combustion of bio and fossil fuels in winter. In spring & summer months, the long range transported dust also adds up with local emissions.

- 4- $\square^{15}\text{N}_{\text{PM}2.5}$ values showed significant correlation with ambient NH_3 concentrations for peak winter months (December and January) indicating dominance of secondary formed particulate ammonium sulphates via gas to particle conversion. In post-monsoon and spring-summer months, no such relationship was observed. $\square^{15}\text{N}_{\text{PM}2.5}$ values displayed significant positive correlations with surface solar radiation and ambient temperature indicating importance of amplifications and photolytic destructions of aerosol N species in changing meteorological conditions.
- 5- We surmise that atmospheric NH_3 emissions originating from agricultural fields in the surrounding regions of the New Delhi region are playing major role in the observed atmospheric haziness, under a supportive meteorological condition occurring between late-November to January months. When ambient NH_3 concentrations rose to $>300 \square\text{g.m}^{-3}$ over New Delhi, and if ambient temperatures are rather lower $<20^\circ\text{C}$ amidst higher relative humidity ($>70\text{-}80\%$), episodes of atmospheric haziness (SMOG) could be experienced.
- 6- During the entire study period (post-monsoon, winter and spring-summer), $\square^{34}\text{S}_{\text{PM}2.5}$ values showed signatures of coal-combustion, road dust, typical continental polluted-air and biogenic sulphur. Lowering of $\square^{34}\text{S}_{\text{PM}2.5}$ values during severely degraded air-quality periods, indicate a likely dominance of biogenic sulphur.. $\square^{34}\text{S}_{\text{PM}2.5}$ values also showed significant positive and negative correlations with ambient temperature (& air-visibility) and relative humidity respectively.
- 7- Cluster analysis and concentration weighted wind trajectory analysis for the study period indicated that the winds from northwest of New Delhi (originating from Panjab-Haryana states) contribute $\sim64\%$ and $\sim58\%$ air mass trajectories over New Delhi during the post-monsoon and winter months.

CRediT authorship contribution statement

Ravi Sawlani: Investigation, Data curation, Writing – original draft,

Rajesh Agnihotri:Conceptualization, Resources, Supervision, Writing- review and Editing,

Chhemendra Sharma: Resources, Supervision, Review and Editing

Declaration of competing interest

Authors declare that there is no conflict of interest

Acknowledgements

We thank Directors of CSIR National Physical Laboratory New Delhi and Birbal Sahni Institute of Palaeosciences, Lucknow for facilities. RS thanks DST Inspire fellowship (IF-140084) and The Academy of Scientific and Innovative Research (AcSIR).

References

- Aggarwal, S.G., Kawamura, K., 2008. Molecular distributions and stable carbon isotopic compositions of dicarboxylic acids and related compounds in aerosols from Sapporo, Japan: Implications for photochemical aging during long-range atmospheric transport. *Journal of Geophysical Research* 113. <https://doi.org/10.1029/2007JD009365>
- Aggarwal, S.G., Kawamura, K., Umarji, C.S., Tachibana, E., Patil, R.S., Gupta, P.K., 2013. Organic and inorganic markers and stable C-, N-isotopic compositions of tropical coastal aerosols from megacity Mumbai: sources of organic aerosols and atmospheric processing. *Atmospheric Chemistry and Physics* 13, 4667–4680. <https://doi.org/10.5194/acp-13-4667-2013>
- Agnihotri, R., 2015. Stable Isotopic and Chemical Characteristics of Bulk Aerosols during Winter and Summer Seasons at a Station in Western Coast of India (Goa). *Aerosol and Air Quality Research* 2015. <https://doi.org/10.4209/aaqr.2014.07.0127>
- Agnihotri, R., Kumar, R., Prasad, M.V.S.N., Sharma, C., Bhatia, S.K., Arya, B.C., 2014. Experimental Setup and Standardization of a Continuous Flow Stable Isotope Mass Spectrometer for Measuring Stable Isotopes of Carbon, Nitrogen and Sulfur in Environmental Samples. *MAPAN* 29, 195–205. <https://doi.org/10.1007/s12647-014-0099-8>
- Agnihotri, R., Mandal, T.K., Karapurkar, S.G., Naja, M., Gadi, R., Ahammmmed, Y.N., Kumar, A., Saud, T., Saxena, M., 2011. Stable carbon and nitrogen isotopic composition of bulk aerosols over India and northern Indian Ocean. *Atmospheric Environment* 45, 2828–2835.

<https://doi.org/10.1016/j.atmosenv.2011.03.003>

Amrani, A., Said-Ahmad, W., Shaked, Y., Kiene, R.P., 2013. Sulfur isotope homogeneity of oceanic DMSP and DMS. *Proceedings of the National Academy of Sciences* 110, 18413–18418.
<https://doi.org/10.1073/pnas.1312956110>

An, Z., Huang, R.-J., Zhang, R., Tie, X., Li, G., Cao, J., Zhou, W., Shi, Z., Han, Y., Gu, Z., Ji, Y., 2019. Severe haze in northern China: A synergy of anthropogenic emissions and atmospheric processes. *Proc Natl Acad Sci USA* 116, 8657–8666.
<https://doi.org/10.1073/pnas.1900125116>

Ancelet, T., Davy, P.K., Trompetter, W.J., Markwitz, A., Weatheburn, D.C., 2011. Carbonaceous aerosols in an urban tunnel. *Atmospheric Environment* 45, 4463–4469.
<https://doi.org/10.1016/j.atmosenv.2011.05.032>

Anderson, T.L., 2003. ATMOSPHERIC SCIENCE: Climate Forcing by Aerosol—a Hazy Picture. *Science* 300, 1103–1104. <https://doi.org/10.1126/science.1084777>

B., B., H., P., P., A., 2002. Effects of dicyandiamide, farmyard manure and irrigation on crop yields and ammonia volatilization from an alluvial soil under a rice (*Oryza sativa L.*)-wheat (*Triticum aestivum L.*) cropping system. *Biology and Fertility of Soils* 36, 207–214.
<https://doi.org/10.1007/s00374-002-0528-7>

Badarinath, K.V.S., Kharol, S.K., Sharma, A.R., Krishna Prasad, V., 2009. Analysis of aerosol and carbon monoxide characteristics over Arabian Sea during crop residue burning period in the Indo-Gangetic Plains using multi-satellite remote sensing datasets. *Journal of Atmospheric and Solar-Terrestrial Physics* 71, 1267–1276. <https://doi.org/10.1016/j.jastp.2009.04.004>

Baklanov, A., Grimmond, C.S.B., Carlson, D., Terblanche, D., Tang, X., Bouchet, V., Lee, B., Langendijk, G., Kolli, R.K., Hovsepyan, A., 2018. From urban meteorology, climate and environment research to integrated city services. *Urban Climate* 23, 330–341.
<https://doi.org/10.1016/j.uclim.2017.05.004>

Boutton, T.W., Archer, S.R., Midwood, A.J., Zitzer, S.F., Bol, R., 1998. δ13C values of soil organic carbon and their use in documenting vegetation change in a subtropical savanna ecosystem.

Geoderma 82, 5–41. [https://doi.org/10.1016/S0016-7061\(97\)00095-5](https://doi.org/10.1016/S0016-7061(97)00095-5)

Chang, Y., Zhang, Y.-L., Li, J., Tian, C., Song, L., Zhai, X., Zhang, W., Huang, T., Lin, Y.-C., Zhu, C., Fang, Y., Lehmann, M.F., Chen, J., 2019. Isotopic constraints on the atmospheric sources and formation of nitrogenous species in clouds influenced by biomass burning. *Atmos. Chem. Phys.* 19, 12221–12234. <https://doi.org/10.5194/acp-19-12221-2019>

Charlson, R.J., Langner, J., Rodhe, H., 1990. Sulphate aerosol and climate. *Nature* 348, 22–22. <https://doi.org/10.1038/348022a0>

Chowdhury, S., Dey, S., Guttikunda, S., Pillarisetti, A., Smith, F.R., Di Girolamo, L., 2019. Indian annual ambient air quality standard is achievable by completely mitigating emissions from household sources. *Proceedings of the National Academy of Sciences* 116, 10711–10716. <https://doi.org/10.1073/pnas.1900888116>

Chowdhury, Z., Zheng, M., Schauer, J.J., Sheesley, R., Salmon, L.G., Cass, G.R., Russell, A.G., 2007. Speciation of ambient fine organic carbon particles and source apportionment of PM_{2.5} in Indian cities. *Journal of Geophysical Research* 112. <https://doi.org/10.1029/2007JD008386>

Dai, S., Bi, X., Chan, L.Y., He, J., Wang, S., Wang, X., Peng, P., Sheng, G., Fu, J., 2015. Chemical and stable carbon isotopic composition of PM_{2.5} from on-road vehicle emissions in the PRD region and implications for vehicle emission control policy. *Atmospheric Chemistry and Physics* 15, 3097–3103. <https://doi.org/10.5194/acp-15-3097-2015>

Datta, A., Sharma, S.K., Narit, R.C., Kumar, V., Mandal, T.K., Pathak, H., 2012. Ammonia emission from subtropical crop land area in India. *Asia-Pacific J Atmos Sci* 48, 275–281. <https://doi.org/10.1007/s13143-012-0027-1>

David Felix, J., Elliott, E.M., Gish, T.J., McConnell, L.L., Shaw, S.L., 2013. Characterizing the isotopic composition of atmospheric ammonia emission sources using passive samplers and a combined oxidation-bacterial denitrifier approach: Improved method for isotope characterization of ammonia in air. *Rapid Communications in Mass Spectrometry* 27, 2239–2246. <https://doi.org/10.1002/rcm.6679>

Dockery, D.W., Pope, C.A., Xu, X., Spengler, J.D., Ware, J.H., Fay, M.E., Ferris, B.G., Speizer, F.E.,

1993. An Association between Air Pollution and Mortality in Six U.S. Cities. New England Journal of Medicine 329, 1753–1759. <https://doi.org/10.1056/NEJM199312093292401>

Galloway, J.N., Aber, J.D., Erisman, J.W., Seitzinger, S.P., Howarth, R.W., Cowling, E.B., Cosby, B.J., 2003. The Nitrogen Cascade. BioScience 53, 341. [https://doi.org/10.1641/0006-3568\(2003\)053\[0341:TNC\]2.0.CO;2](https://doi.org/10.1641/0006-3568(2003)053[0341:TNC]2.0.CO;2)

Gao, N., Cheng, M.D. and Hopke, P.K., 1993. Potential Source Contribution Function Analysis and Source Apportionment of Sulfur Species Measured at Rubidoux, CA during the Southern California Air Quality Study, 1987. *Anal. Chim. Acta.*, 277: 369–380.

Ghosh, S., Biswas, J., Guttikunda, S., Roychowdhury, S. and Nayak, M., 2015. An investigation of potential regional and local source regions affecting fine particulate matter concentrations in Delhi, India. *J. Air Waste Manage. Assoc.* 65: 218–231

Griffith, S.M., Huang, X.H.H., Louie, P.K.K., Yu, J.Z. 2015. Characterizing the thermodynamic and chemical composition factors controlling PM 2.5 nitrate: Insights gained from two years of online measurements in Hong Kong. *Atmospheric Environment* 122, 864–875.
<https://doi.org/10.1016/j.atmosenv.2015.02.009>

Hallquist, M., Wenger, J.C., Baltensperger, U., Rudich, Y., Simpson, D., Claeys, M., Dommen, J., Donahue, N.M., George, C., Goldstein, A.H., Hamilton, J.F., Herrmann, H., Hoffmann, T., Iinuma, Y., Jang, M., Jenkin, M.E., Jimenez, J.L., Kiendler-Scharr, A., Maenhaut, W., McFiggans, G., Mentel, Th.F., Monod, A., Prévôt, A.S.H., Seinfeld, J.H., Surratt, J.D., Szmigielski, R., Wildt, J., 2009. The formation, properties and impact of secondary organic aerosol: current and emerging issues. *Atmospheric Chemistry and Physics* 9, 5155–5236.
<https://doi.org/10.5194/acp-9-5155-2009>

Han, X., Guo, Q., Liu, C., Fu, P., Strauss, H., Yang, J., Hu, J., Wei, L., Ren, H., Peters, M., Wei, R., Tian, L., 2016. Using stable isotopes to trace sources and formation processes of sulfate aerosols from Beijing, China. *Scientific Reports* 6. <https://doi.org/10.1038/srep29958>

Harris, E., Sinha, B., Hoppe, P., Crowley, J.N., Ono, S., Foley, S., 2012. Sulfur isotope fractionation during oxidation of sulfur dioxide: gas-phase oxidation by OH radicals and aqueous oxidation

by H₂O₂, O₃ and iron catalysis. *Atmospheric Chemistry and Physics* 12, 407–423.

<https://doi.org/10.5194/acp-12-407-2012>

Harrison, R.M., Yin, J., 2000. Particulate matter in the atmosphere: which particle properties are important for its effects on health? *Science of The Total Environment* 249, 85–101.

[https://doi.org/10.1016/S0048-9697\(99\)00513-6](https://doi.org/10.1016/S0048-9697(99)00513-6)

Hoering, T., 1957. The isotopic composition of the ammonia and the nitrate ion in rain. *Geochimica et Cosmochimica Acta* 12, 97–102. [https://doi.org/10.1016/0016-7037\(57\)90021-2](https://doi.org/10.1016/0016-7037(57)90021-2)

Hsu, Y.-K., Holsen, T.M., Hopke, P.K., 2003a. Comparison of hybrid receptor models to locate PCB sources in Chicago. *Atmospheric Environment* 37, 545–562. [https://doi.org/10.1016/S1352-2310\(02\)00886-5](https://doi.org/10.1016/S1352-2310(02)00886-5)

Hsu, Y.-K., Holsen, T.M., Hopke, P.K., 2003b. Locating and Quantifying PCB Sources in Chicago: Receptor Modeling and Field Sampling. *Environmental Science & Technology* 37, 681–690. <https://doi.org/10.1021/es025531x>

Jamieson, R.E., Wadleigh, M.A., 2000. Tracing sources of precipitation sulfate in eastern Canada using stable isotopes and trace metals. *Journal of Geophysical Research: Atmospheres* 105, 20549–20556. <https://doi.org/10.1029/2000JD900249>

Kawamura, K., Kobayashi, M., Tsiboukuma, N., Mochida, M., Watanabe, T., Lee, M., 2004. Organic and inorganic compositions of marine aerosols from East Asia: Seasonal variations of water-soluble dicarboxylic acids, major ions, total carbon and nitrogen, and stable C and N isotopic composition, in: *The Geochemical Society Special Publications*. Elsevier, pp. 243–265. [https://doi.org/10.1016/S1873-9881\(04\)80019-1](https://doi.org/10.1016/S1873-9881(04)80019-1)

Kiehl, J.T., Schneider, T.L., Rasch, P.J., Barth, M.C., Wong, J., 2000. Radiative forcing due to sulfate aerosols from simulations with the National Center for Atmospheric Research Community Climate Model, Version 3. *Journal of Geophysical Research: Atmospheres* 105, 1441–1457. <https://doi.org/10.1029/1999JD900495>

Kirkevåg, A., Iversen, T., Dahlback, A., 1999. On radiative effects of black carbon and sulphate aerosols. *Atmospheric Environment* 33, 2621–2635. [https://doi.org/10.1016/S1352-2310\(98\)00309-4](https://doi.org/10.1016/S1352-2310(98)00309-4)

- Krishna Prasad, V., Badarinath, K., 2006. Soil surface nitrogen losses from agriculture in India: A regional inventory within agroecological zones (2000–2001). International Journal of Sustainable Development & World Ecology 13, 173–182.
<https://doi.org/10.1080/13504500609469670>
- Krouse, H.R., Grinenko, V.A., International Council of Scientific Unions, United Nations Environment Programme (Eds.), 1991. Stable isotopes: natural and anthropogenic sulphur in the environment, SCOPE. Published on behalf of the Scientific Committee on Problems of the Environment (SCOPE) of the International Council of Scientific Unions (ICSU) in collaboration with the United Nations Environment Programme by Wiley, Chichester ; New York.
- Kundu, S., Kawamura, K., Lee, M., 2010. Seasonal variation of the concentrations of nitrogenous species and their nitrogen isotopic ratios in aerosols at Gosan, Jeju Island: Implications for atmospheric processing and source changes of aerosols. Journal of Geophysical Research 115. <https://doi.org/10.1029/2009JD013323>
- Liu, N., Yu, Y., He, J., Zhao, S., 2013. Integrated modeling of urban-scale pollutant transport: application in a semi-arid urban valley, Northwestern China. Atmospheric Pollution Research 4, 306–314. <https://doi.org/10.5194/APR.2013.034>
- Liu, X., Zhang, Y., Han, W., Tang, A., Shen, J., Cui, Z., Vitousek, P., Erisman, J.W., Goulding, K., Christie, P., Fangmeier, A., Zhang, F., 2013. Enhanced nitrogen deposition over China. Nature 494, 459– 62. <https://doi.org/10.1038/nature11917>
- López-Veneroni, D., 2009. The stable carbon isotope composition of PM_{2.5} and PM₁₀ in Mexico City Metropolitan Area air. Atmospheric Environment 43, 4491–4502.
<https://doi.org/10.1016/j.atmosenv.2009.06.036>
- Malm, W.C., Molenar, J.V., Eldred, R.A., Sisler, J.F., 1996. Examining the relationship among atmospheric aerosols and light scattering and extinction in the Grand Canyon area. Journal of Geophysical Research: Atmospheres 101, 19251–19265. <https://doi.org/10.1029/96JD00552>
- Mast, M.A., Turk, J.T., Ingersoll, G.P., Clow, D.W., Kester, C.L., 2001. Use of stable sulfur isotopes to identify sources of sulfate in Rocky Mountain snowpacks. Atmospheric Environment 35,

3303–3313. [https://doi.org/10.1016/S1352-2310\(00\)00507-0](https://doi.org/10.1016/S1352-2310(00)00507-0)

McGowan, H., Clark, A., 2008. Identification of dust transport pathways from Lake Eyre, Australia using Hysplit. *Atmospheric Environment* 42, 6915–6925.
<https://doi.org/10.1016/j.atmosenv.2008.05.053>

Meng, Z., Xu, X., Lin, W., Ge, B., Xie, Y., Song, B., Jia, S., Zhang, R., Peng, W., Wang, Y., Cheng, H., Yang, W., Zhao, H., 2018. Role of ambient ammonia in particulate ammonium formation at a rural site in the North China Plain. *Atmos. Chem. Phys.* 18, 167–184.
<https://doi.org/10.5194/acp-18-167-2018>

Narukawa, M., Kawamura, K., Li, S.-M., Bottenheim, J.W., 2005. Stable carbon isotopic ratios and ionic composition of the high-Arctic aerosols: An increase in $\delta^{13}\text{C}$ values from winter to spring. *Journal of Geophysical Research* 113. <https://doi.org/10.1029/2007JD008755>

Nielsen, H., 1974. Isotopic composition of the major contributors to atmospheric sulfur. *Tellus* 26, 213–221. <https://doi.org/10.1111/j.2153-3490.1974.tb01969.x>

Norman, A.L., Barrie, L.A., Toom-Sauntry, D., Sirois, A., Krouse, H.R., Li, S.M., Sharma, S., 1999. Sources of aerosol sulphate at Alert: Apportionment using stable isotopes. *Journal of Geophysical Research: Atmospheres* 104, 11619–11631.
<https://doi.org/10.1029/1999JD900078>

Newman, L., and J. Forrest, Sulphur isotope measurements relevant to power plant emissions in the northeastern United States, in *Stable Isotopes: Natural and Anthropogenic Sulphur in the Environment*, SCOP-43, edited by H. R. Krouse and V. A. Grinenko, pp. 331- 343, John Wiley, New York, 1991.

Pan, Y., Tian, S., Liu, D., Fang, Y., Zhu, X., Zhang, Q., Zheng, B., Michalski, G., Wang, Y., 2016a. Fossil Fuel Combustion-Related Emissions Dominate Atmospheric Ammonia Sources during Severe Haze Episodes: Evidence from ^{15}N -Stable Isotope in Size-Resolved Aerosol Ammonium. *Environmental Science & Technology* 50, 8049–8056.
<https://doi.org/10.1021/acs.est.6b00634>

Pathak, H., Li, C., Wassmann, R., Ladha, J.K., 2006. Simulation of Nitrogen Balance in Rice-Wheat Systems of the Indo-Gangetic Plains. *Soil Sci. Soc. Am. J.* 70, 1612–1622.

<https://doi.org/10.2136/sssaj2005.0165>

Pavuluri, C.M., Kawamura, K., Tachibana, E., Swaminathan, T., 2010. Elevated nitrogen isotope ratios of tropical Indian aerosols from Chennai: Implication for the origins of aerosol nitrogen in South and Southeast Asia. *Atmospheric Environment* 44, 3597–3604.
<https://doi.org/10.1016/j.atmosenv.2010.05.039>

Plautz, J., 2018. Ammonia, a poorly understood smog ingredient, could be key to limiting deadly pollution. *Science*. <https://doi.org/10.1126/science.aav3862>

Pokhrel, A., Kawamura, K., Seki, O., Matoba, S., Shiraiwa, T., 2015. Ice core profiles of saturated fatty acids (C 12:0 –C 30:0) and oleic acid (C 18:1) from southern Alaska since 1734 AD: A link to climate change in the Northern Hemisphere. *Atmospheric Environment* 100, 202–209.
<https://doi.org/10.1016/j.atmosenv.2014.11.007>

Pope, C.A., Dockery, D.W., 2006. Health Effects of Fine Particulate Air Pollution: Lines that Connect. *Journal of the Air & Waste Management Association* 56, 709–742.
<https://doi.org/10.1080/10473289.2005.10464485>

Pope III, C.A., 2002. Lung Cancer, Cardiopulmonary Mortality, and Long-term Exposure to Fine Particulate Air Pollution. *JAMA* 287, 1132. <https://doi.org/10.1001/jama.287.9.1132>

Pöschl, U., 2005. Atmospheric Aerosols: Composition, Transformation, Climate and Health Effects. *Angewandte Chemie International Edition* 44, 7520–7540.
<https://doi.org/10.1002/anie.200501122>

Qi, M., Jiang, L., Liu, Y., Xiong, Q., Sun, C., Li, X., Zhao, W., Yang, X., 2018. Analysis of the Characteristics and Sources of Carbonaceous Aerosols in PM2.5 in the Beijing, Tianjin, and Langfang Region, China. *International Journal of Environmental Research and Public Health* 15, 1483. <https://doi.org/10.3390/ijerph15071483>

Ramana, M.V., Ramanathan, V., Podgorny, I.A., Pradhan, B.B., Shrestha, B., 2004. The direct observations of large aerosol radiative forcing in the Himalayan region: AEROSOL RADIATIVE FORCING OVER THE HIMALAYAN REGION. *Geophysical Research Letters* 31, n/a-n/a. <https://doi.org/10.1029/2003GL018824>

Rastogi, N., Agnihotri, R., Sawlani, R., Patel, A., Babu, S.S., Satish, R., 2020. Chemical and isotopic characteristics of PM10 over the Bay of Bengal: Effects of continental outflow on a marine environment. *Science of The Total Environment* 726, 138438.
<https://doi.org/10.1016/j.scitotenv.2020.138438>

Reinmuth-Selzle, K., Kampf, C.J., Lucas, K., Lang-Yona, N., Fröhlich-Nowoisky, J., Shiraiwa, M., Lakey, P.S.J., Lai, S., Liu, F., Kunert, A.T., Ziegler, K., Shen, F., Sgarbanti, R., Weber, B., Bellinghausen, I., Saloga, J., Weller, M.G., Duschl, A., Schuppan, D., Pöschl, U., 2017. Air Pollution and Climate Change Effects on Allergies in the Anthropocene: Abundance, Interaction, and Modification of Allergens and Adjuvants. *Environmental Science & Technology* 51, 4119–4141. <https://doi.org/10.1021/es704908>

Romero, A.B., 2003. Mass-independent sulfur isotopic compositions in present-day sulfate aerosols. *Journal of Geophysical Research* 108. <https://doi.org/10.1029/2003JD003660>

Rudolph, J., Anderson, R.S., v. Czapiewski, K., Czuća, E., Ernst, D., Gillespie, T., Huang, L., Rigby, C., Thompson, A.E., 2003. [No title found]. *Journal of Atmospheric Chemistry* 44, 39–55.
<https://doi.org/10.1023/A:1022116304550>

Saltzman, E.S., Brass, G.W., Price, D.A., 1983. The mechanism of sulfate aerosol formation: Chemical and sulfur isotopic evidence. *Geophysical Research Letters* 10, 513–516.
<https://doi.org/10.1029/GL010i007p00513>

Sawlani, R., Agnihotri, R., Sharma, C., Patra, P.K., Dimri, A.P., Ram, K., Verma, R.L., 2019. The severe Delhi SMOG of 2016: A case of delayed crop residue burning, coincident firecracker emissions, and atypical meteorology. *Atmospheric Pollution Research* 10, 868–879.
<https://doi.org/10.1016/j.apr.2018.12.015>

Seinfeld, J.H., Pandis, S.N., 2016. *Atmospheric chemistry and physics: from air pollution to climate change*, Third edition. ed. John Wiley & Sons, Hoboken, New Jersey.

Sharma, M., Kishore, S., Tripathi, S.N., Behera, S.N., 2007. Role of atmospheric ammonia in the formation of inorganic secondary particulate matter: A study at Kanpur, India. *Journal of Atmospheric Chemistry* 58, 1–17. <https://doi.org/10.1007/s10874-007-9074-x>

Singh, A., Dey, S., 2012. Influence of aerosol composition on visibility in megacity Delhi.

Atmospheric Environment 62, 367–373. <https://doi.org/10.1016/j.atmosenv.2012.08.048>

Sirois, A., Bottenheim, J.W., 1995. Use of backward trajectories to interpret the 5-year record of PAN and O₃ ambient air concentrations at Kejimkujik National Park, Nova Scotia. *Journal of Geophysical Research* 100, 2867. <https://doi.org/10.1029/94JD02951>

Stein, A.F., Draxler, R.R., Rolph, G.D., Stunder, B.J.B., Cohen, M.D., Ngan, F., 2015. NOAA's HYSPLIT Atmospheric Transport and Dispersion Modeling System. *Bulletin of the American Meteorological Society* 96, 2059–2077. <https://doi.org/10.1175/BAMS-D-14-00110.1>

Subramanian, M., 2016. Can Delhi save itself from its toxic air? *Nature* 534, 166–169.
<https://doi.org/10.1038/534166a>

Sun, Y., Jiang, Q., Wang, Z., Fu, P., Li, J., Yang, T., Yin, Y., 2014. Investigation of the sources and evolution processes of severe haze pollution in Beijing in January 2013: Sources and Evolution of Haze Pollution. *J. Geophys. Res. Atmos.* 119, 4380–4398.
<https://doi.org/10.1002/2014JD02141>

Takigawa, M., Patra, P.K., Matsumi, Y., Dhaka, S.K., Nakayama, T., Yamaji, K., Kajino, M., Hayashida, S., 2020. Can Delhi's Pollution be Affected by Crop Fires in the Punjab Region? *SOLA* 16, 86–91. <https://doi.org/10.2151/sola.2020-015>

Tiwari, S., Payra, S., Mohar, M., Verma, S., Bisht, D.S., 2011. Visibility degradation during foggy period due to anthropogenic urban aerosol at Delhi, India. *Atmospheric Pollution Research* 2, 116–120. <https://doi.org/10.5094/APR.2011.014>

Tostevin, R., Turchyn, A.V., Farquhar, J., Johnston, D.T., Eldridge, D.L., Bishop, J.K.B., McIlvin, M., 2014. Multiple sulfur isotope constraints on the modern sulfur cycle. *Earth and Planetary Science Letters* 396, 14–21. <https://doi.org/10.1016/j.epsl.2014.03.057>

Turekian, V.C., Macko, S., Ballentine, D., Swap, R.J., Garstang, M., 1998. Causes of bulk carbon and nitrogen isotopic fractionations in the products of vegetation burns: laboratory studies. *Chemical Geology* 152, 181–192. [https://doi.org/10.1016/S0009-2541\(98\)00105-3](https://doi.org/10.1016/S0009-2541(98)00105-3)

Wang, Y., Chen, J., Wang, Q., Qin, Q., Ye, J., Han, Y., Li, L., Zhen, W., Zhi, Q., Zhang, Y., Cao, J., 2019. Increased secondary aerosol contribution and possible processing on polluted winter

- days in China. *Environment International* 127, 78–84.
<https://doi.org/10.1016/j.envint.2019.03.021>
- Wang, G., Zhang, R., Gomez, M.E., Yang, L., Levy Zamora, M., Hu, M., Lin, Y., Peng, J., Guo, S., Meng, J., Li, J., Cheng, C., Hu, T., Ren, Y., Wang, Yuesi, Gao, J., Cao, J., An, Z., Zhou, W., Li, G., Wang, J., Tian, P., Marrero-Ortiz, W., Secrest, J., Du, Z., Zheng, J., Shang, D., Zeng, L., Shao, M., Wang, W., Huang, Y., Wang, Yuan, Zhu, Y., Li, Y., Hu, J., Pan, B., Cai, L., Cheng, Y., Ji, Y., Zhang, F., Rosenfeld, D., Liss, P.S., Duce, R.A., Kolb, C.E., Molina, M.J., 2016. Persistent sulfate formation from London Fog to Chinese haze. *Proceedings of the National Academy of Sciences* 113, 13630–13635. <https://doi.org/10.1073/pnas.1616540113>
- Wang, Y., Zhuang, G., Zhang, X., Huang, K., Xu, C., Tang, A., Chen, J., An, Z., 2006. The ion chemistry, seasonal cycle, and sources of PM_{2.5} and TSP aerosol in Shanghai. *Atmospheric Environment* 40, 2935–2952. <https://doi.org/10.1016/j.atmosenv.2005.12.051>
- Wang, Y.Q., Zhang, X.Y., Draxler, R.R., 2009. TrajStat: GIS-based software that uses various trajectory statistical analysis methods to identify potential sources from long-term air pollution measurement data. *Environmental Modelling & Software* 24, 938–939.
<https://doi.org/10.1016/j.envsoft.2009.01.004>
- Widory, D., 2007. Nitrogen isotopes: Tracers of origin and processes affecting PM10 in the atmosphere of Paris. *Atmospheric Environment* 41, 2382–2390.
<https://doi.org/10.1016/j.atmosenv.2006.11.009>
- Widory, D., 2006. Combustibles, fuels and their combustion products: A view through carbon isotopes. *Combustion Theory and Modelling* 10, 831–841.
<https://doi.org/10.1080/13647830600720264>
- Wu,D.; Liu,Q.; Lian, Y.; Bi, X.; Li, F.; Tan,H.; Liao, B.; Chen,H., 2012. Hazyweather formation and visibility deterioration resulted from fine particulate (PM2.5) pollutions in Guangdong and Hong Kong. *J. Environ. Sci. Circumst.*, 32,2660–2669.
- Xing, Y.-F., Xu, Y.-H., Shi, M.-H., Lian, Y.-X., 2016. The impact of PM2.5 on the human respiratory system. *J Thorac Dis* 8, E69-74. <https://doi.org/10.3978/j.issn.2072-1439.2016.01.19>
- Zhang, J.J., Samet, J.M., 2015. Chinese haze versus Western smog: lessons learned. *J Thorac Dis* 7,

3–13. <https://doi.org/10.3978/j.issn.2072-1439.2014.12.06>

Figure Captions-

Figure 1: Locations of Delhi on Indian map (A) and aerosol-sampling site on map of Delhi (B). Panels C, E and G show fire-count data for post-monsoon, winter and spring-summer months, respectively. Panel D, F and H show typical MODIS images representing these meteorologically distinct periods.

Figure 2: Measured variability in mass concentrations of PM_{2.5}, TC, TN and TS and their isotopic compositions over New Delhi between September 2014 to May 2015. PM_{2.5} and TC concentrations enhanced right after the post-monsoon (harvesting) season, while winter months were obviously dominated by enhanced N and S particulate concentrations and appear responsible for enhanced PM_{2.5} loadings.

Figure 3: Monthly variability (A) Mass concentrations of PM_{2.5} and TC with monthly mean ambient temperature and relative humidity (RH) (B) Mass concentrations of TN and TS with ambient monthly mean concentrations of trace gases (NH₃, NO_x and SO₂) over central New Delhi.

Figure 4: (A) Significant covariance between ambient NH₃ and aerosol TN concentrations for post-monsoon to winter months (Oct to Feb) reveal gaseous N₂O₃ emissions significantly contributing to particulate TN component of aerosols over New Delhi via gas to particulate conversions. (B) □¹⁵N_{PM2.5} show a significant correlation with ambient NH₃ concentrations only during peak winter months (Dec to Feb).

Figure 5: Box-whisker plots of δ¹³C_{PM2.5}, δ¹⁵N_{PM2.5}, and δ³⁴S_{PM2.5} values observed for post-monsoon, winter and spring-summer months shown along with average value of typical source isotopic values.

a Rudolph et al., 2003; b Agnihotri et al., 2011; c Turekian et al., 1998; d Sawlani et al., 2019; e Widory et al., 2007; f Pavuluri et al., 2010; g Hoering et al., 1957; h Amrani et al., 2013; i Norman et al., 1999; j Tostevin et al., ; k Mast et al., 2001

Figure 6: Monthly variability (A) Mass concentrations of PM_{2.5}, TC, TN and TS with monthly means of surface solar radiation (watt.m⁻²) and air-visibility data (B) Box-whiskers of aerosol □¹⁵N values showing influences of optical parameters of air-quality. Likewise, (C) Box-whiskers of aerosol □³⁴S values showed noticeable influences of ambient temperature and relative humidity.

Figure 7: Ambient NH₃ converting to particulate fraction TN (of PM2.5) under enhanced relative humidity resulting in atmospheric haziness (A). Panel B clearly shows enhanced NH₃ levels (> ~300 □g.m⁻³) resulting in poor air-visibility days for New Delhi under declined ambient temperatures.

Figure 8: India map, showing the mean wind trajectory path of six identified clusters (Fig. 8A-C). Concentration weighted wind trajectory (CWT) for New Delhi are shown in Fig. 8 D-F.

Table 1: Average mass concentrations of PM_{2.5} mass, C, N, S, and their stable isotopic ratios along with trace gases (NH₃, NO_x and SO₂) and MET (relative humidity and temperature) parameters in total range observed over period of collection during September 2014 to May 2015 periods.

Season		PM _{2.5}	[TN]	[TC]	[TS]	□ ¹⁵ N	□ ¹³ C	□ ³⁴ S	NOx	SO ₂	NH ₃	RH	TEMP	SSR.	AIR VIS
Post-Monsoon (Sept, Oct, Nov; n = 27)	Mean	193.8	12.9	97.6	13.5	7.73	-26.0	3.5	56.1	18.1	121.7	57.6	26.6	284.2	1.6
	Std. dev	99.4	7.2	53.4	11.6	4.10	0.8	2.0	40.0	8.03	72.8	40.0	3.8	84.6	0.6
Winter (Dec, Jan, Feb; n = 52)	Mean	219.9	23.7	100.0	20.6	7.32	-25.6	3.1	62.3	32.1	214.6	75.3	18.8	280.0	0.8
	Std. dev	93.2	13.6	42.5	15.6	6.61	1.8	1.1	35.4	25.0	114.2	15.3	3.70	75.1	0.3
Summer (Mar, Apr, May; n = 38)	Mean	135.6	4.5	61.4	4.0	12.3	-25.1	3.8	62.7	65.4	40.7	48.2	30.5	404.8	1.5
	Std. dev	54.7	1.4	18.8	3.6	4.6	3.4	0.8	34.8	25.9	23.2	17.36	4.92	90.6	0.4

Graphical abstract

Highlights

- First aerosol C, N and S isotopic composition data of PM_{2.5} over New Delhi
- Highest PM_{2.5} concentrations found during winter months due to vigorous N and S cycling
- TC+TN+TS contents of PM_{2.5} inhibit surface solar radiation and deteriorate air-visibility
- Aerosol $\square^{15}\text{N}$ linearly increase with ambient NH₃ concentrations during winter amidst declined temperatures
- ~64 and ~58% of air mass over New Delhi for post-monsoon and winter months is contributed by winds from Panjab-Haryana

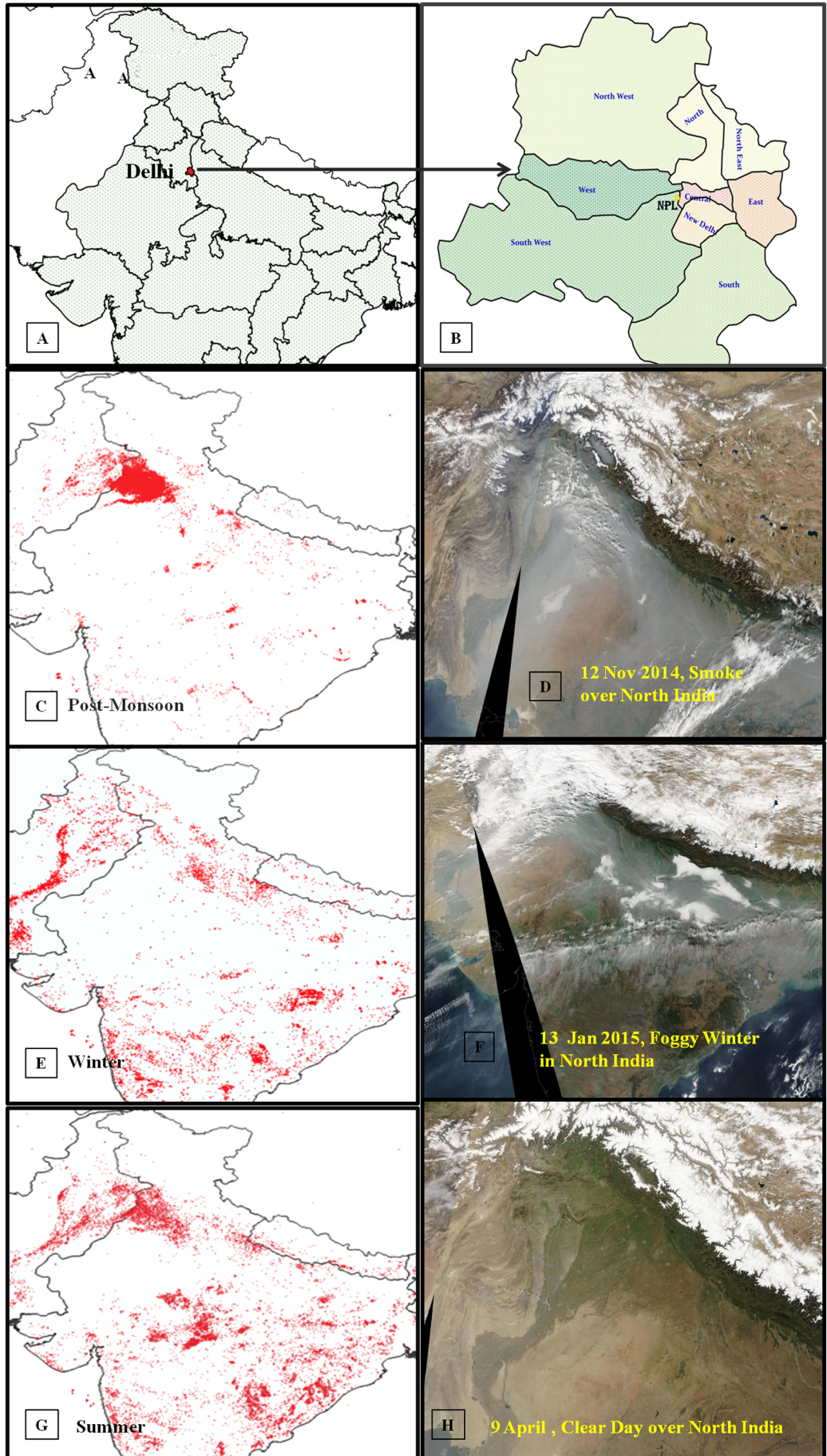


Figure 1

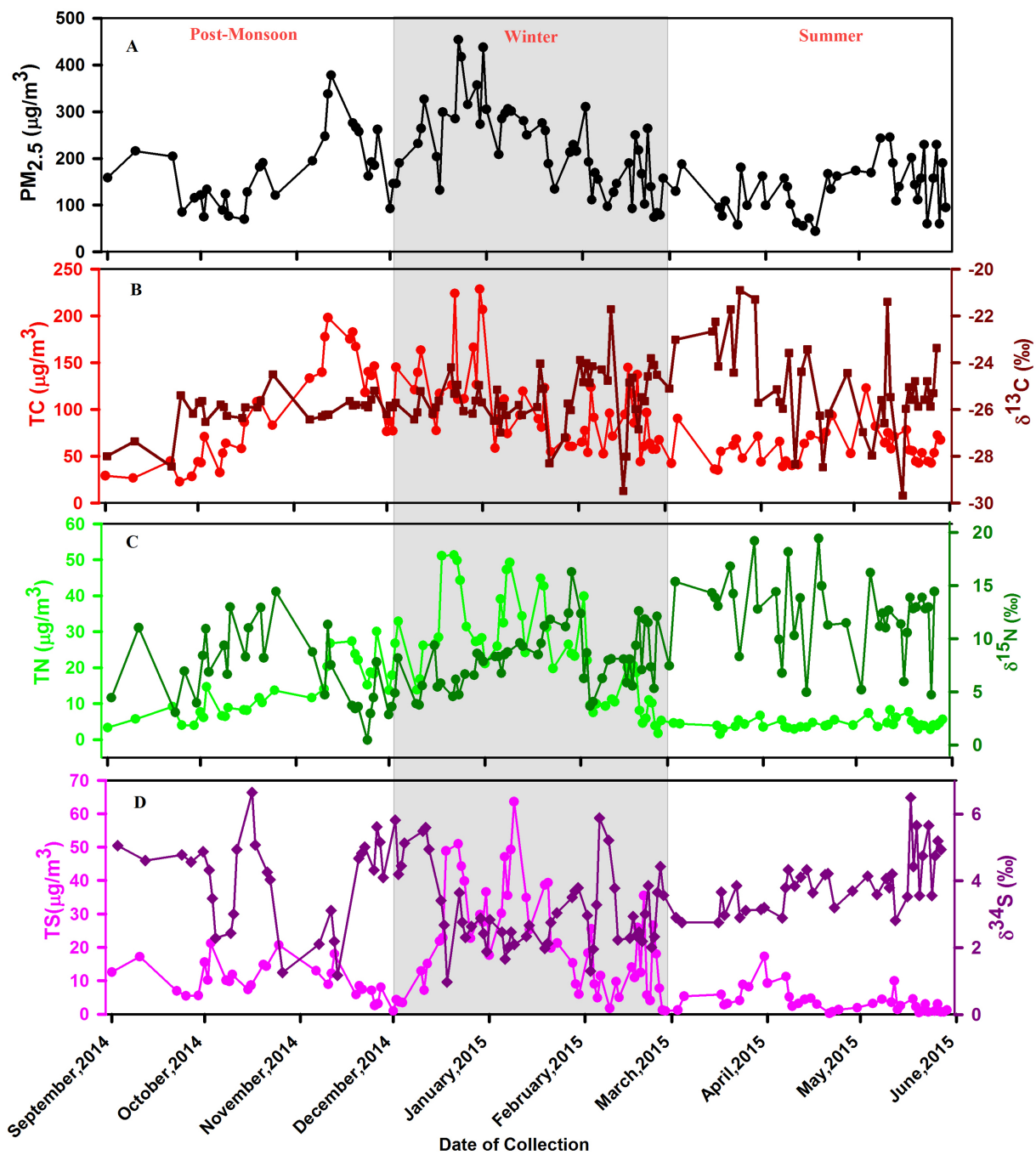


Figure 2

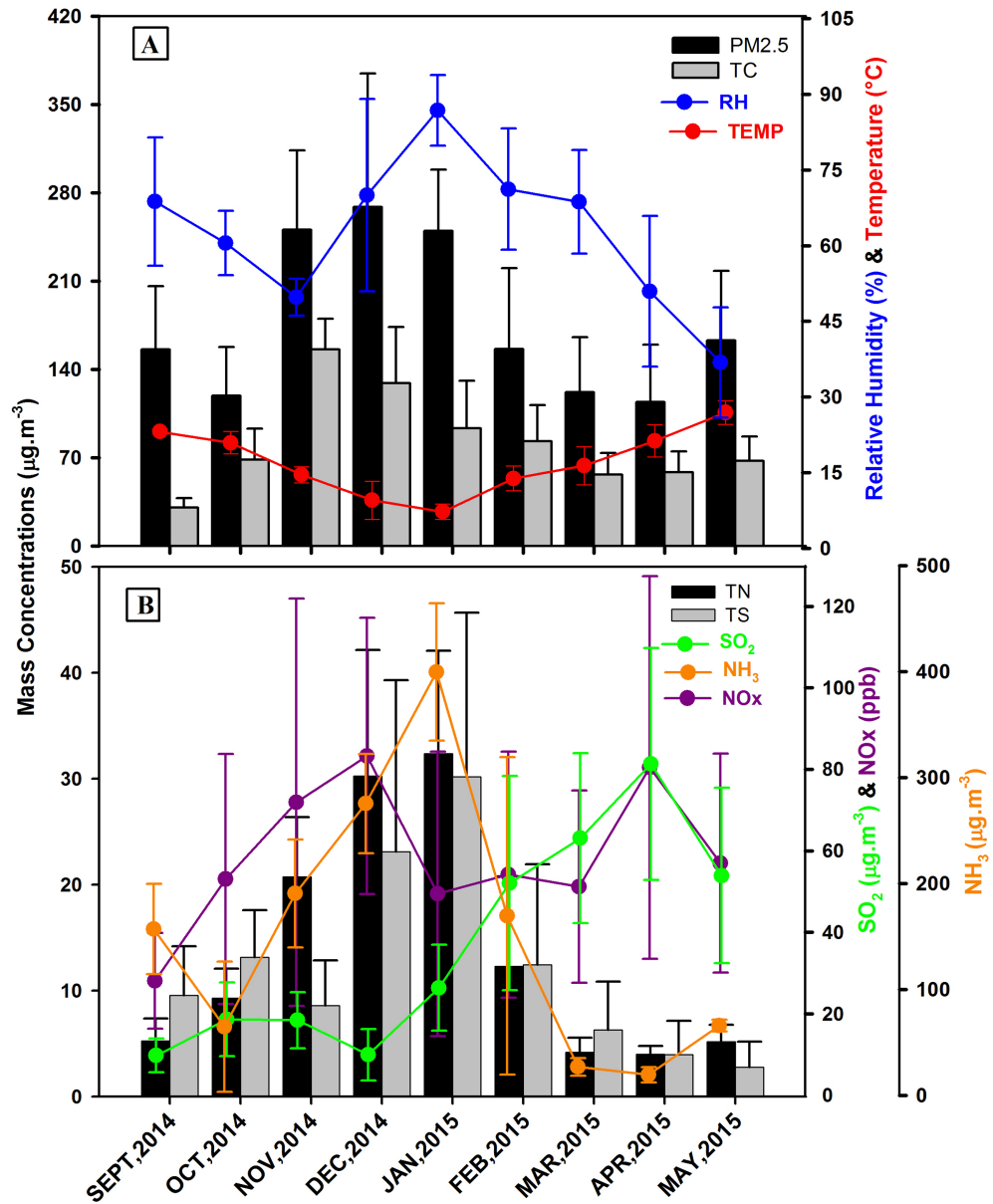


Figure 3

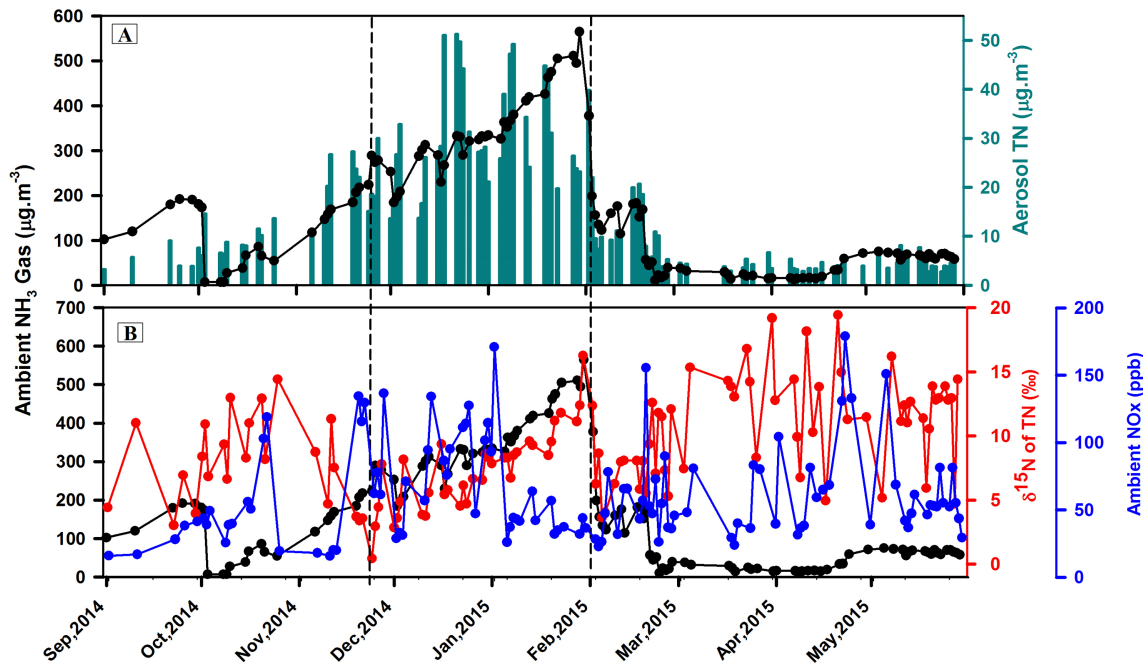


Figure 4

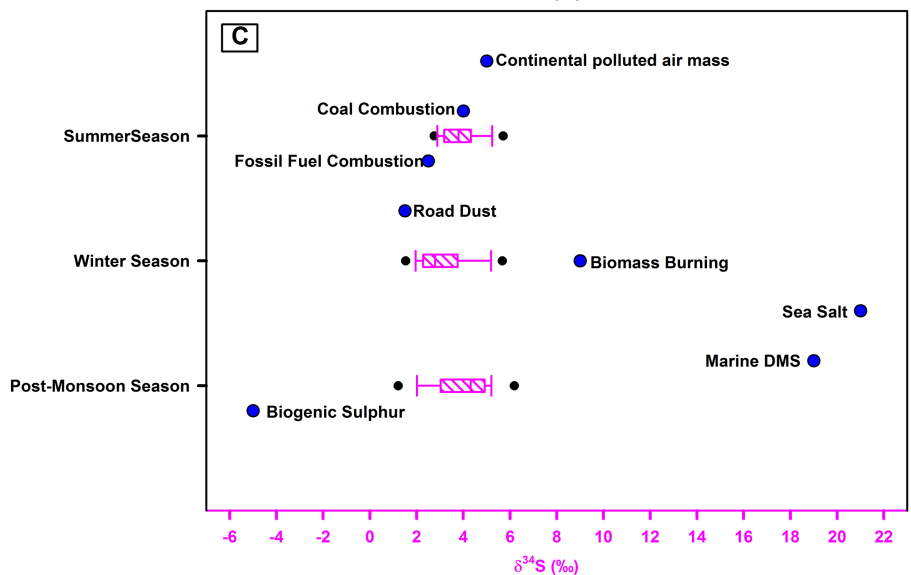
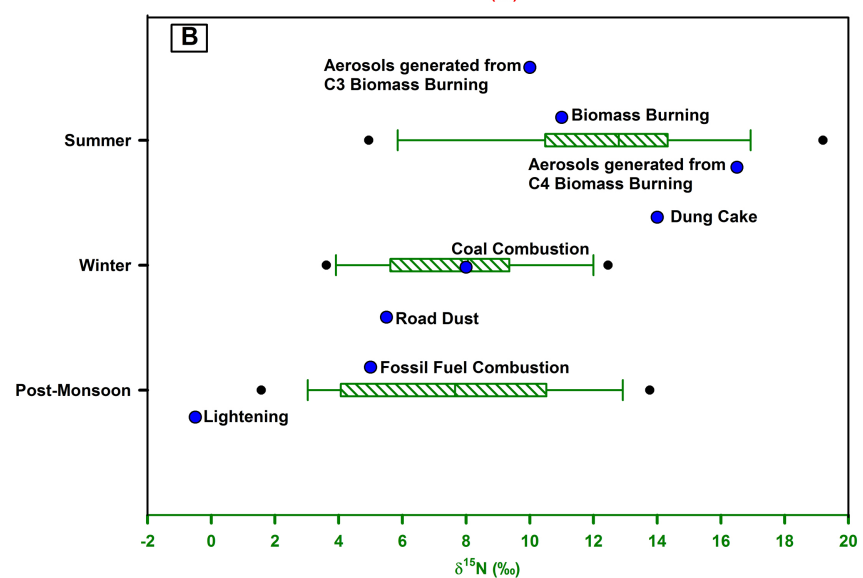
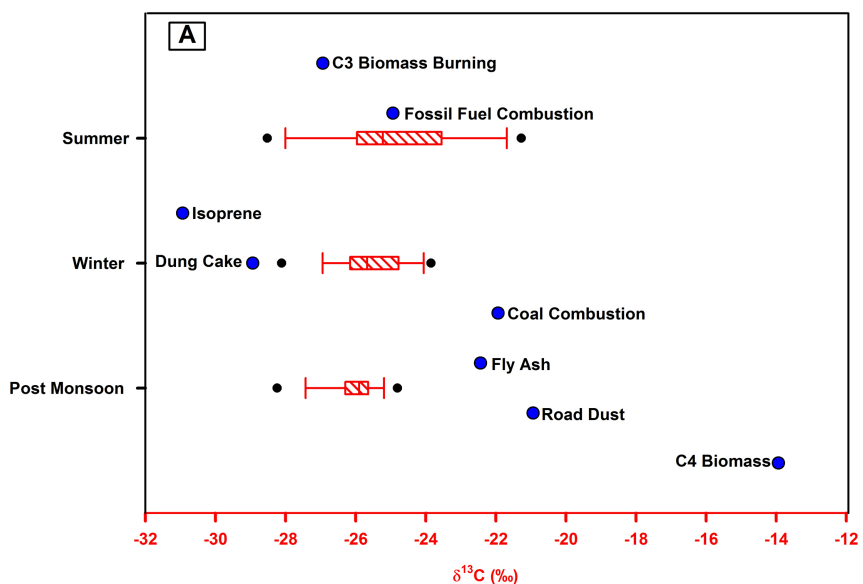


Figure 5

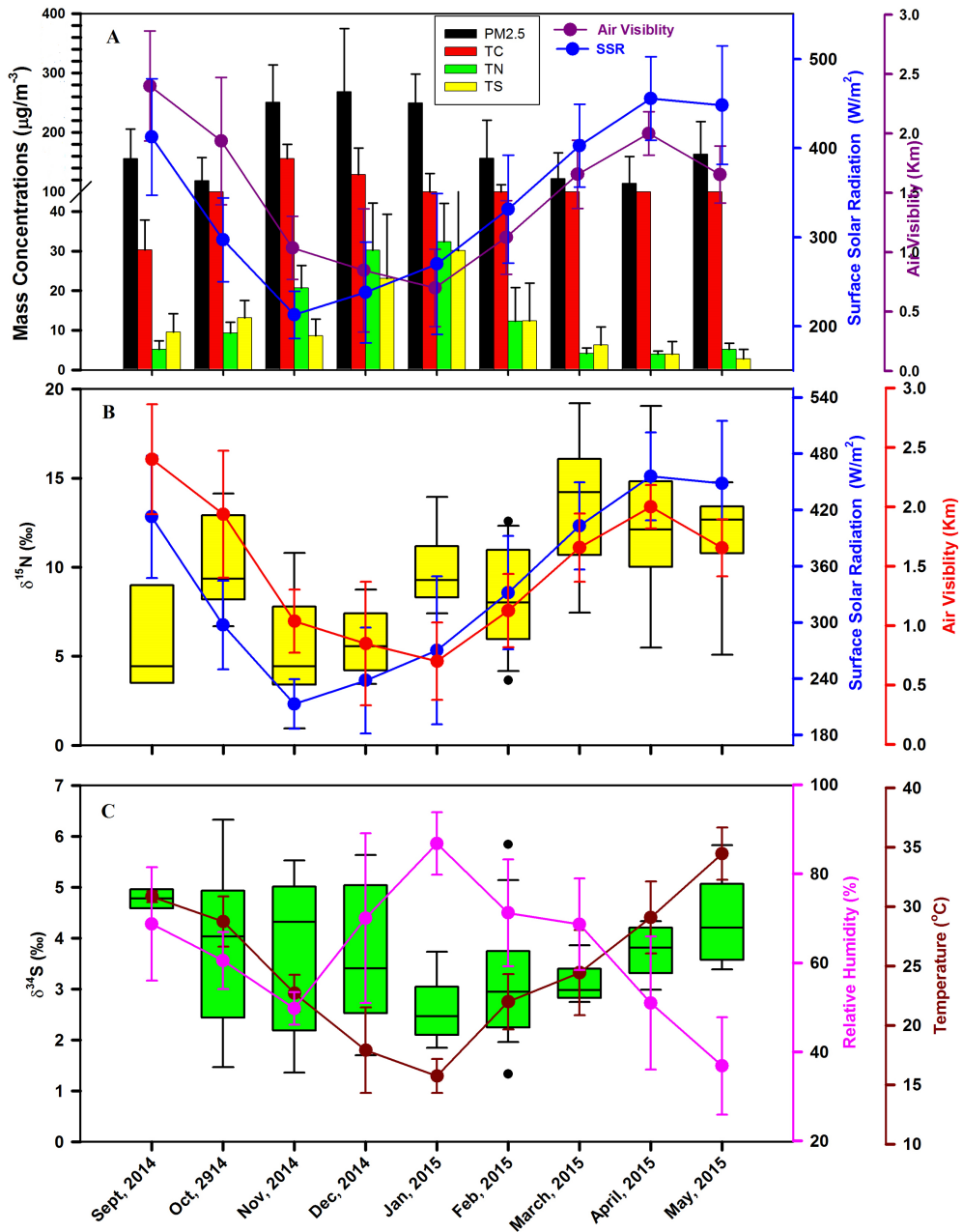


Figure 6

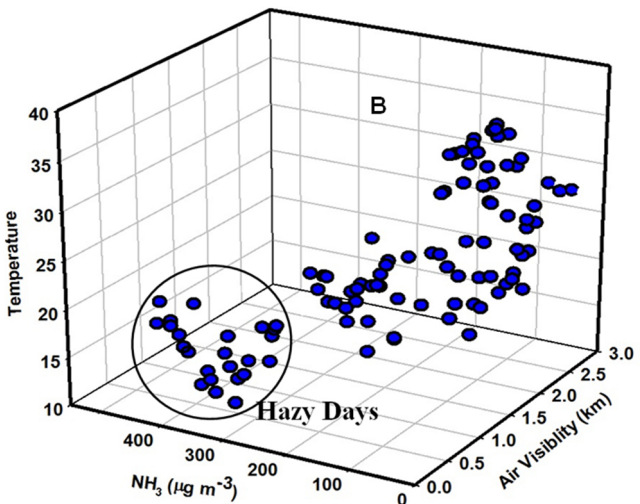
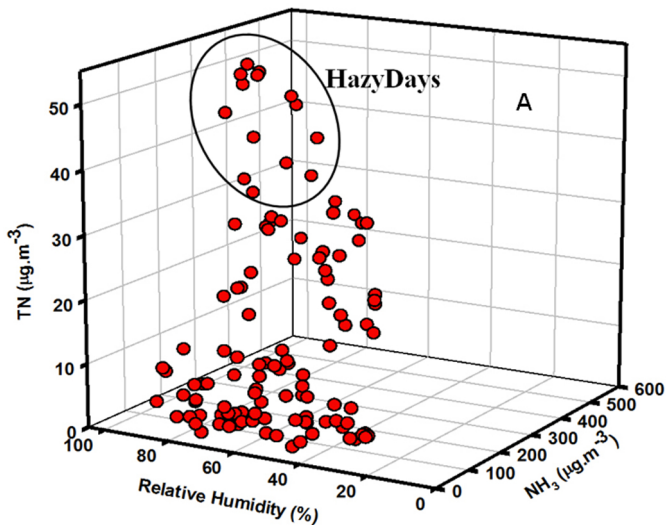


Figure 7

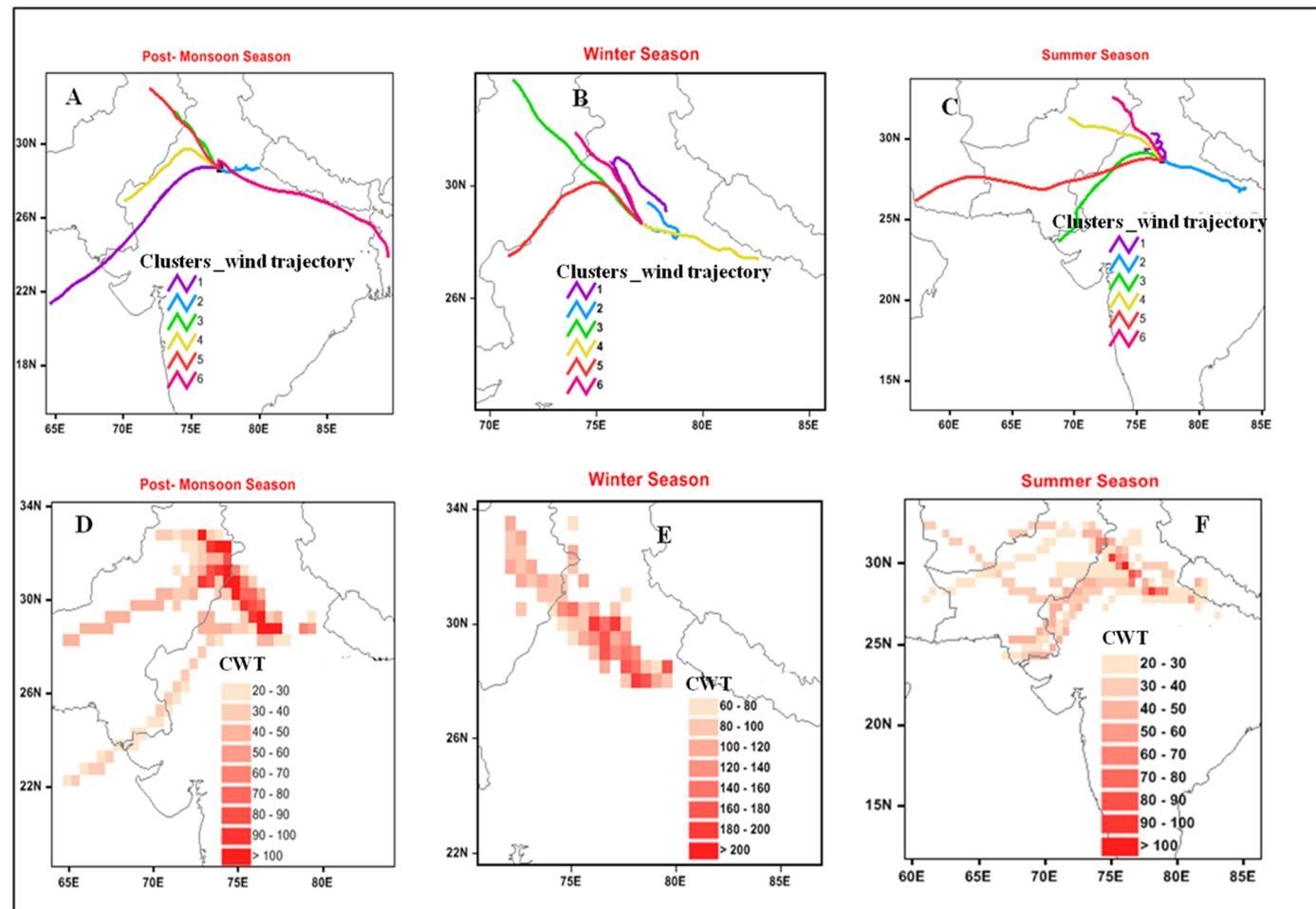


Figure 8